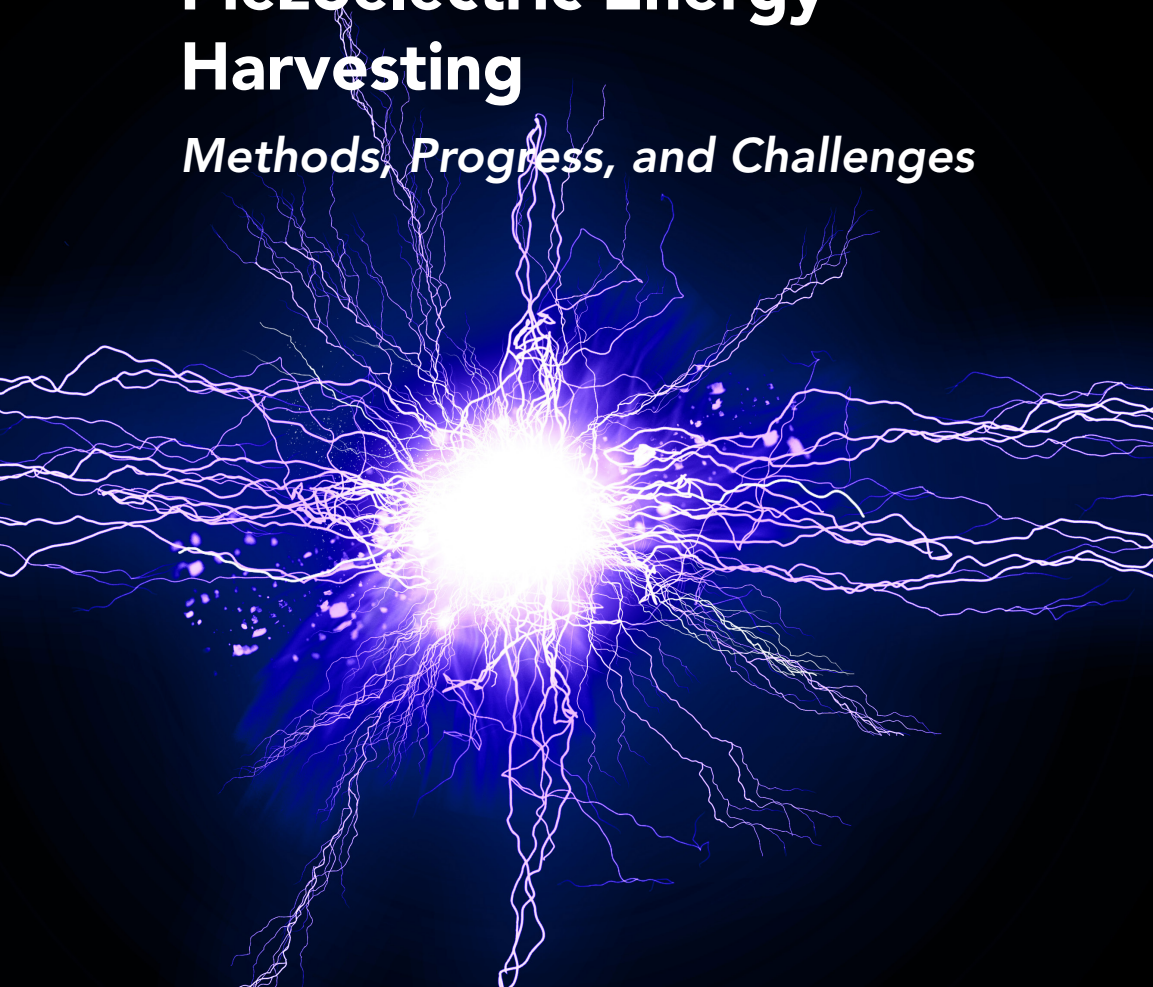


# ENERGY PHYSICS AND ENGINEERING COLLECTION

Jonathan Swingler, *Editor*

## **Piezoelectric Energy Harvesting**

*Methods, Progress, and Challenges*



**Mohammad Adnan Ilyas**



**MOMENTUM PRESS  
ENGINEERING**

# **PIEZOELECTRIC ENERGY HARVESTING**



# **PIEZOELECTRIC ENERGY HARVESTING**

**METHODS, PROGRESS, AND CHALLENGES**

**MOHAMMAD ADNAN ILYAS**



**MOMENTUM PRESS  
ENGINEERING**

**MOMENTUM PRESS, LLC, NEW YORK**

*Piezoelectric Energy Harvesting: Methods, Progress, and Challenges*

Copyright © Momentum Press®, LLC, 2018.

All rights reserved. No part of this publication may be reproduced, stored in a retrieval system, or transmitted in any form or by any means—electronic, mechanical, photocopy, recording, or any other—except for brief quotations, not to exceed 400 words, without the prior permission of the publisher.

First published by Momentum Press®, LLC  
222 East 46th Street, New York, NY 10017  
[www.momentumpress.net](http://www.momentumpress.net)

ISBN-13: 978-1-94561-270-1 (print)  
ISBN-13: 978-1-94561-271-8 (e-book)

Momentum Press Energy Physics and Engineering Collection

Cover and interior design by Exeter Premedia Services Private Ltd.,  
Chennai, India

10 9 8 7 6 5 4 3 2 1

Printed in the United States of America

# ABSTRACT

Environmental pollution has been one of the main challenges for sustainable development. Piezoelectric materials can be used as a means of transforming ambient vibrations into electrical energy to power devices. The focus is on an alternative approach to scavenge energy from the environment. This book presents harvesting methodologies to evaluate the potential effectiveness of different techniques and provides an overview of the methods and challenges of harvesting energy using piezoelectric materials.

Piezoelectric energy harvesters have many applications, including sensor nodes, wireless communication, microelectromechanical systems, handheld devices, and mobile devices. The book also presents a new approach within piezoelectric energy harvesting using the impact of rain drops. The energy harvesting model presented is further analyzed for single-unit harvester and an array of multiple harvesters to maximize the efficiency of the device.

## KEYWORDS

autonomous systems, efficiency, Energy harvesting, piezoelectric, PVDF, PZT, raindrop, reliability



# CONTENTS

<b>LIST OF FIGURES</b>	<b>ix</b>
<b>LIST OF TABLES</b>	<b>xi</b>
<b>1 INTRODUCTION</b>	<b>1</b>
<b>2 ENERGY HARVESTING</b>	<b>3</b>
2.1 Context	3
2.2 Autonomous Energy Systems	4
2.3 Vibrational Energy Harvesting	6
2.4 Thermoelectric Energy Harvesting	10
2.5 Photovoltaic Energy Harvesting	13
2.6 Combined Energy Harvesting	14
<b>3 PIEZOELECTRICITY</b>	<b>17</b>
3.1 Background Theory	17
3.2 Piezoelectric Materials	18
<b>4 PIEZOELECTRIC ENERGY HARVESTING TECHNIQUES</b>	<b>23</b>
4.1 Modeling	23
4.2 Mechanical and Electrical Behavior	25
4.3 Circuit Topologies	25
4.4 Experimental Work	26
<b>5 RAINDROP ENERGY HARVESTING</b>	<b>31</b>
5.1 Review of Publications	31
5.2 Characteristics of a Harvester	34
5.3 Experimental Investigation	39

<b>6 CONCLUSION</b>	<b>47</b>
6.1 Challenges	47
6.2 Future Prospects	48
<b>REFERENCES</b>	<b>49</b>
<b>ABOUT THE AUTHOR</b>	<b>55</b>
<b>INDEX</b>	<b>57</b>

# LIST OF FIGURES

Figure 2.1. Block diagram for an autonomous energy harvesting system.	5
Figure 2.2. Model of a vibration energy harvester.	6
Figure 2.3. Circuit diagram of an electromagnetic generator.	7
Figure 2.4. Circuit diagram of an electrostatic generator.	8
Figure 2.5. Circuit diagram of a piezoelectric generator.	10
Figure 2.6. Model adaptation of Seebeck effect.	11
Figure 2.7. Block diagram of a TEG.	12
Figure 2.8. Circuit diagram of a PV cell.	13
Figure 3.1. Structure of piezo crystals.	18
Figure 4.1. Cantilever arrangement with mass.	25
Figure 4.2. Equivalent circuit model for piezoelectric energy harvester.	26
Figure 4.3. Full-wave bridge rectifier.	27
Figure 4.4. Full-bridge rectifier and voltage doubler connected to piezoelectric energy harvester.	27
Figure 4.5. Mass versus output voltage at no load.	28
Figure 4.6. Output power against resistive load.	29
Figure 5.1. Water droplet impact on solid surface.	35
Figure 5.2. Impact zones for water droplets on a piezo device.	39
Figure 5.3. Voltage output and sensor position profiles of the device (Taken from [80]).	40
Figure 5.4. Voltage output of harvester for an impact (Taken from [80]).	40
Figure 5.5. Voltage against load for a single device (Taken from [80]).	41
Figure 5.6. Voltage and power profiles of a single device (Taken from [80]).	42
Figure 5.7. Voltage and peak power the module with multiple devices (Taken from [83]).	43



# LIST OF TABLES

Table 2.1. Power consumption of various battery-operated devices	3
Table 2.2. Energy sources with their harvested power density	5
Table 2.3. Comparison of energy densities	10
Table 2.4. Advantages and disadvantages of transducers	11
Table 3.1. Materials with piezoelectric constant	19
Table 4.1. Output voltage at various loads	28
Table 4.2. Power parameters for compressions	28
Table 4.3. Power parameters for linear motion	29
Table 5.1. Raindrop size versus terminal velocity (Taken from [80])	38



## CHAPTER 1

---

# INTRODUCTION

Governments around the world look for ways to boost economies, with an emphasis on multidisciplinary research and business–academic collaboration. This involves investment that will be focused on science, research, and innovation, with development of a number of priority technologies. The focus for governments and legislators will be on delivering affordable and clean energy growth. The growth in the energy sector is constantly under review to ensure new technologies are developed locally. As an example, the UK government identified smart, flexible, and clean energy technologies as one of the key areas in which to become the global lead by solving the energy challenge of supplying clean, affordable energy securely to ever more-demanding societies around the world.

Over the next few decades, making better use of energy resources will be just as important as finding alternative sources of supply. Development of new technologies becomes more important as the country’s demand for energy keeps growing. Conventional technologies may have high efficiencies in meeting the demand, but have a significant impact on the environment and resources. The use of fossil fuels in conventional technologies is likely to continue for the foreseeable future, but significant progress has been made in decreasing the carbon dioxide emission. The need for novel energy harvesting technologies within the renewable energy sector has become important than ever. Research within the field of energy harvesting has attracted a lot of attention in recent years by scavenging low-grade ambient energy sources, such as environmental vibrations and human power into usable electrical energy. Such devices are, therefore, potentially attractive as replacements for primary batteries in low-power electronics.

This book has been put together for students, researchers, and scientists working in the field of energy harvesting systems. It brings together a review of energy harvesting methods, with a focus on piezoelectric

energy harvesting. The book demonstrates the current progress within piezoelectric energy harvesting and challenges faced within the field. This introductory chapter presents the rationale and emphasis of the book.

Chapter 2 lays out the fundamental concept of autonomous energy systems, with a focus on energy harvesting. The chapter further gives a brief overview of various harvesting techniques and technologies widely used ranging from vibrational to photovoltaic.

Chapter 3 introduces the background theory with piezoelectricity and gives the reader an overview of various fabricated or commercially available piezoelectric materials for energy harvesting systems.

Chapter 4 looks at the various techniques and empirically models a piezoelectric energy harvester. It also discusses different circuit topologies and efficiency of such systems. The study of piezoelectric energy harvesting is the focal point of the book.

Chapter 5 introduces a novel technique to harvest energy using raindrop impacts on a piezoelectric device. The chapter gives an in-depth review of publications within the field of raindrop energy harvesting, which only has a handful researchers currently work on this theme.

## CHAPTER 2

---

# ENERGY HARVESTING

## 2.1 CONTEXT

Batteries are in wide use for many devices or systems depending on their functionality, which makes us highly dependent on batteries as the power source to power such devices. Even though batteries have proven to be a good source of power, they have a few weaknesses mainly due to size, weight, safety, and life. Emerging applications like wireless micro-sensor networks [1] and micro electromechanical systems (MEMS) [2] are a couple of examples of such emerging technologies that could integrate energy harvesting technologies to provide power. Replacing batteries in such devices becomes difficult because of the complexity and size. A favorable solution to power-up such devices would be to have a battery-less operation. We can scavenge energy from the environment through energy harvesting concepts to support such battery-less operations.

Many portable or handheld devices, such as MP3 players, hearing aid, and pacemaker, are all operated by batteries. Types of batteries used in such devices vary from lithium-ion batteries to alkaline batteries. In many cases, the battery life is limited to days or months, which is not always ideal. Table 2.1: Power consumption of various battery-operated devices

**Table 2.1.** Power consumption of various battery-operated devices

Device	Power consumption
Smartphone	1W
MP3 player	50mW
Hearing aid	1mW
Wireless sensor node	100 $\mu$ W
Cardiac pacemaker	50 $\mu$ W
Quartz watch	5 $\mu$ W

shows the typical power consumption of such devices that generally can be as little as in the  $\mu\text{W}$  range [3].

Energy harvesting is a renewable form of power generation, which has the potential to power handheld devices, implantable medical devices, health monitoring devices, and sensors. Recently, research on energy harvesting has attracted tremendous attention as green energy becomes a hot issue. The challenge is to provide efficient and *clean* power for micro- to macro-level applications. Solar, vibrational, or thermal energy is the most common source of energy used for harvesting. There are many energy fields available from which to harvest energy:

- Radiation (light, solar, electromagnetic radiation)
- Thermal (temperature gradient)
- Mechanical (potential, kinetic)
- Chemical (battery, fuel cell)
- Nuclear
- Magnetic
- Electric

Benefits of energy harvesting can be summarized as:

- Clean and regenerative source of energy
- Long-lasting operability
- Cost saving
- Flexibility
- Maintenance free

## 2.2 AUTONOMOUS ENERGY SYSTEMS

An autonomous energy system can be defined as consisting of three stages: generation, conversion, and consumption. The energy generation stage requires an energy harvesting device along with an energy source or storage technology that could be used to accumulate energy in excess from the harvester and provide it to the system in its place whenever energy is sufficient. The energy conversion stage requires power management circuitry and system that trades and optimizes the energy harvested in the energy generation block to the energy consumption stage. Figure 2.1 represents the stages of an autonomous energy harvesting system.

Various approaches of energy harvesting can be made to power various electronic devices with low power consumption. Table 2.2 represents

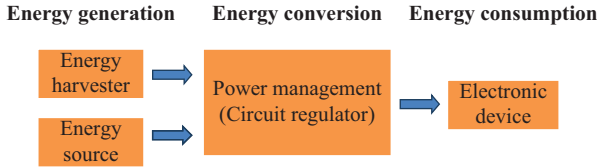


**Figure 2.1.** Block diagram for an autonomous energy harvesting system.

**Table 2.2.** Energy sources with their harvested power density

Source	Harvested power density
<b>Light</b>	
Indoor	$10\mu\text{W}/\text{cm}^2$
Outdoor	$10\text{mW}/\text{cm}^2$
<b>Vibration/Motion</b>	
Human	$4\mu\text{W}/\text{cm}^2$
Industrial	$100\mu\text{W}/\text{cm}^2$
<b>Thermal</b>	
Human	$25\text{--}30\mu\text{W}/\text{cm}^2$
Industrial	$5\text{--}10\text{mW}/\text{cm}^2$

a comparison of harvested power densities using different ambient energy sources as experimentally conducted by various researchers [4, 5, 6].

A significant amount of research has been devoted to developing and understanding power harvesting systems. The idea to develop portable devices and sensors that rely on regenerative source has put the focus of research in the area of power harvesting. Solar, vibrational, or thermal energy is the most common source of energy used for harvesting. Vibrational energy is available just about everywhere in the urban and industrial environment, but it is often overlooked as a source of power to be scavenged. The vibrational harvesters use one of the three methods: electromagnetic, electrostatic, or piezoelectric to harvest energy. Researchers have been successful in testing such generators and transducers, for converting mechanical energy into electrical energy.

Autonomous electrical devices are increasingly being commercialized due to low-power electronics and energy harvesting. Piezoelectric energy harvesting (PEH) is one of the most promising technologies that can harvest ambient vibration or motion. PEHs are well suited to isolated applications where there are sufficient vibrations, but lack of access to

power supplies. It is thought that piezoelectric generators have a very high theoretical and practical energy density in comparison with electromagnetic and electrostatic harvesters. IDTechEx studies have predicted that investment in energy harvesting technologies will grow to a substantial amount, and it is estimated that the market for piezoelectric energy harvesters will reach over 1 billion dollars by 2027 [7].

## 2.3 VIBRATIONAL ENERGY HARVESTING

Mechanical energy sources can be found almost anywhere, and vibration sources such as ocean waves and human motion makes converting mechanical energy into electrical energy an attractive approach. A significant amount of research has been devoted to developing and understanding power harvesting systems. The idea to develop portable devices and sensors that rely on regenerative source has put the focus of research in the area of power harvesting. Vibrational energy is available just about everywhere in the urban and industrial environment, but it is often overlooked as a source of power to be scavenged. The vibrational harvesters use one of three methods: electromagnetic, electrostatic or piezoelectric to harvest energy. Researchers have been successful in testing such generators, sensors, actuators, and transducers for converting mechanical energy into electrical energy.

Many researchers have designed mechanical to electrical energy devices based on different conversion mechanisms. Such a mechanism can be defined as a simple kinetic energy harvester first developed by Williams and Yates [8] as adapted in Figure 2.2. The generator consists of a seismic mass,  $m$ , on a spring with a spring constant of  $k$ , and  $b$  is the damping coefficient that consists of mechanically and electrically induced

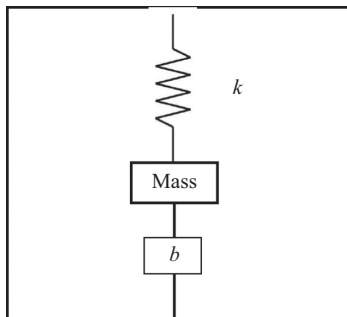


**Figure 2.2.** Model of a vibration energy harvester.

damping coefficient. As the generator vibrates, the mass moves out of phase with the generator housing. This net movement can drive a suitable transducer to generate electrical energy.

### 2.3.1 ELECTROMAGNETIC

In 1831, electromagnetic induction was discovered by Michael Faraday. Faraday's law of electromagnetic induction pretty much defines the working principle of most electrical motors, generators, and transformers. Faraday's law states that any change in the magnetic field of a coil will cause voltage to be induced, which is referred to as electromotive force (emf). Figure 2.3 shows the circuit representation of an electromagnetic generator where  $R_c$  and  $R_L$  are resistances of the coil and load, respectively, and  $L_c$  is the inductance of the coil.

Voltage induced in the coil can be determined by Faraday's law and can be written as [9]:

$$emf = K \frac{dz}{dt} \quad (2.1)$$

where  $K$  is a constant (described by turns in a coil, length, area, shape, and magnetic field intensity).

The open circuit voltage can be determined by:

$$V_{oc} = NBl \frac{dx}{dt} \quad (2.2)$$

where  $N$  is the number of turns in coil,  $B$  is the magnetic induction,  $l$  is the length of windings, and  $x$  is the relative displacement between the magnet and the coil.

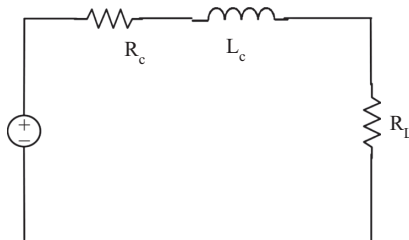


**Figure 2.3.** Circuit diagram of an electromagnetic generator.

### 2.3.2 ELECTROSTATIC

An electrostatic generator relies on the variable capacitor that is driven by mechanical vibrations. As the charge in the capacitor gets constrained, it moves from the capacitor to the load. This way the mechanical energy is converted into electrical energy.

An adaptation of the circuit diagram representation of an electrostatic generator [10] is shown in Figure 2.4 where  $C_V$  is the variable capacitor and  $C_L$  is the load. The maximum voltage across the load can be defined, but we need to define other parameters first.

Capacitance can be defined as:

$$C = Q / V \quad (2.3)$$

where  $Q$  is the charge on the plates and  $V$  is the voltage on the plates.

For a parallel plate capacitor,  $C$  is given by:

$$C = \frac{\epsilon_0 \epsilon_r A}{d_s} \quad (2.4)$$

where  $\epsilon_0$  is the dielectric permittivity of free space,  $\epsilon_r$  is the relative dielectric permittivity of the material between the capacitor plates,  $A$  is the area of the capacitor plates, and  $d_s$  is the distance between the plates.

Electrostatic generators consist of a capacitor related to the displacement. Equation 2.5 can be deduced for current [9]:

$$I = V_o \frac{dC(z)}{dt} + C(z) \frac{dV}{dt} \quad (2.5)$$

where  $V$  is the voltage when capacitor is charged,  $V_o$  is the initial voltage, and  $C$  is the capacitance.

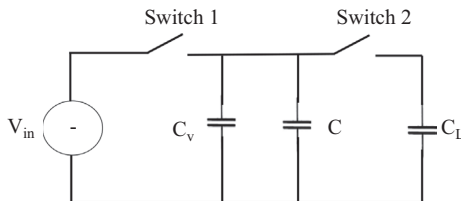


**Figure 2.4.** Circuit diagram of an electrostatic generator.

### 2.3.3 PIEZOELECTRIC

Piezoelectric harvesters consist of an active dielectric material, the piezoelectric, which is plated with a conductor or has an arrangement of a conductor to capture the electric charge developed due to mechanical displacement.

PEH devices use vibrations, motion, or acoustic sound as the source of external energy, which can be converted into electrical energy. These are typically used for application with low-power requirements, such as powering sensor equipment from ambient vibrations [11], MEMS [12], wireless sensors [13], and military applications [14]. Although significant progress has been made in this field in the development of micro-scale power supplies, power management, and consumption, there remains a need to improve these further with the advent of the *Internet of Things*.

The piezoelectric effect was discovered by Pierre and Currie in 1880. A piezoelectric material is capable of producing an electric charge when the material undergoes mechanical stress. There are many materials, such as quartz and tourmaline crystals, that exhibit this piezoelectric effect. Such materials have, in the past, been actively used as electromechanical transducers [15]. The ferroelectric group of materials that exhibit the piezoelectric effect are also known as piezoelectric materials. Ferroelectric ceramics, such as lead zirconate titanate (PZT), are widely used in EH due to their favorable properties, and much discussion can be found in the literature on these, for example [16, 17]. PZT devices have been considered to be a prospective replacement for batteries in some applications due to their high piezoelectric character and energy output. Organic materials such as polyvinylidene fluoride (PVDF) are mainly used in applications requiring a higher degree of mechanical flexibility and optical transparency. These polymers are relatively cheap and can be easily integrated into various applications: in garments or shoes [18]. These polymers also exhibit unique features such as demonstrating excellent mechanical behavior, being corrosion-resistant, having the ability to withstand stress without structural fatigue, and illustrating an ease of processability on dielectric thin films. In particular, these polymers have the potential to be integrated into flexible devices [19].

Figure 2.5 represents the circuit diagram of a piezoelectric generator, where  $R_s$  denotes the resistance of the piezoelectric material,  $C$  is the capacitance, and  $R_L$  is the resistive load.

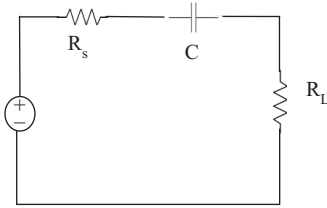


**Figure 2.5.** Circuit diagram of a piezoelectric generator.

### 2.3.4 SUMMARY OF GENERATORS

Previous studies have found that piezoelectric generators are, by far, the most advantageous and can yield up to  $35.4\text{mJ}/\text{cm}^3$  of energy density. Table 2.3 gives a comparison of the energy densities of the three vibration-based generators achieved practically and theoretically [20]. Piezoelectric generators are considered to have high power output and efficiency, but require a higher frequency.

Table 2.4 gives an overview of the advantages and disadvantages of different transducers (electrostatic, electromagnetic, and piezoelectric) as published by researchers [21, 22, 23].

## 2.4 THERMOELECTRIC ENERGY HARVESTING

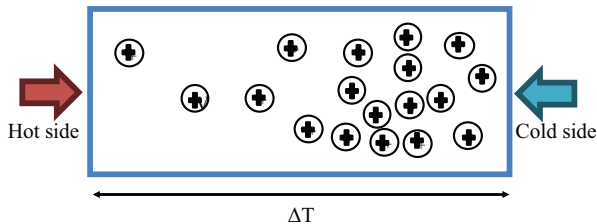
The phenomenon used by thermoelectric devices was introduced by Thomas J. Seebeck in 1821. When a temperature difference is created in a material, due to charged particle movement, an electric potential is created between the ends of the material. In simple terms, this ratio of electric potential and temperature difference is defined as the Seebeck effect, as represented in Figure 2.6. The positivity of Seebeck effect depends on the material, where the positive Seebeck effect denotes electrons being the dominant charge in the material, and negative sign denotes the holes are dominant in the material.

**Table 2.3.** Comparison of energy densities

	Practical ( $\text{mJ}/\text{cm}^3$ )	Theoretical ( $\text{mJ}/\text{cm}^3$ )
Piezoelectric	35.4	335
Electrostatic	4	44
Electromagnetic	24.8	400

**Table 2.4.** Advantages and disadvantages of transducers

	Advantages	Disadvantages
Electrostatic	Small size Control of mechanical resonance	Requires separate voltage source Higher frequency than piezoelectric is needed Low output current
Electromagnetic	No voltage source required Higher power output	Complex design Difficult to integrate into microsystems
Piezoelectric	Simple design No voltage source required Higher power output Small size High efficiency Precise mechanical control	Needs higher frequency Limited material selection Poor mechanical properties Low output current

**Figure 2.6.** Model adaptation of Seebeck effect.

Usually, thermoelectric materials are used for thermoelectric modules where a single couple or many couples are formed together. One side of the module cools down, while the other heats up, and this effect is reversible. The Seebeck coefficient is a number describing the voltage produced between two points on a conductor, where a uniform temperature difference of 1K exists between the points.

A thermoelectric converter obeys laws of thermodynamics just like an ordinary heat engine. Figure of merit ( $ZT$ ) is defined as the measure of the efficiency of thermoelectric materials and is given by the following expression:

$$ZT = \frac{\alpha^2}{K\rho} T \quad (2.6)$$

where  $T$  is temperature in Kelvin,  $\alpha$  is the Seebeck coefficient,  $K$  is the thermal conductivity, and  $\rho$  is the electrical resistivity.

$ZT$  is a measure of the material efficiency and can be decreased with passive heat losses in a device. Thermoelectric phenomenon exists in all conducting materials, with the exception of superconductors. Only those materials that possess a figure of merit greater than 0.5 are usually regarded as thermoelectric materials. There are many thermoelectric materials available, and researchers have conducted various studies to increase the electrical conduction and decrease thermal conduction of these materials. This can be achieved easily by doping them with other useful alloys or materials. A couple of well-known thermoelectric materials include: Bismuth Telluride with an efficiency in a thermoelectric device at around 15 percent [24] and solid solution of  $Mg_2B^{IV}$  compounds where  $B^{IV}$  denotes either silicon (Si), germanium (Ge), or tin (Sn) with a high figure of merit at 1.1 [25].

A block diagram of a thermoelectric generator (TEG) is shown in Figure 2.7. TEG normally consists of an n- and p-type semiconductor materials connected together. TEG uses thermocouples, which are made out of crystalline semiconductor material. Passing heat through this material generates a voltage across the thermocouples, thus causing current to circulate in a closed ring across a load. The device turns into an electric power supply as a voltage difference develops between the top and bottom strips. This arrangement simply acts as a TEG.

Voltage from the semiconductor thermocouple remains low, and in practice, a number of thermocouples are connected electrically in series and thermally parallel by sandwiching them between two ceramic plates. The ceramic plates have high thermal conductivity and low electrical conductivity. A TEG can produce practical electricity to run household appliances such as vacuum cleaners, power tools, lighting, and similar items.

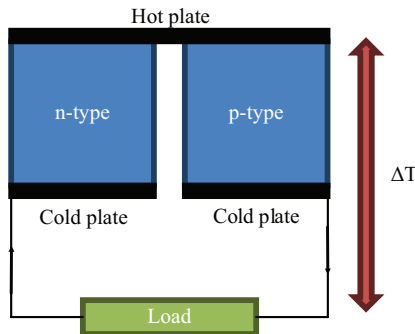


**Figure 2.7.** Block diagram of a TEG.

The TEG is virtually silent, with no noise, environmentally friendly, reliable, and has many advantages and practical applications. Previous studies have shown an increase in the development of small generators for aerospace and military applications [26] and an increasing interest in waste heat recovery using various heat sources such as industrial heat-generating processes [27]. TEGs have also been fabricated for converting human body heat energy into electrical energy with the use of polydimethylsiloxane (PDMS) and generated up to 50nW at a temperature gradient of 7°C [28].

## 2.5 PHOTOVOLTAIC ENERGY HARVESTING

Photovoltaic (PV) systems use cells to convert daylight into electricity. Light is almost universally available, making PV generators feasible to generate electrical energy. PV cells are cheaper than other generators or harvesters currently available. The cells are generally made up of layers of semiconducting material to enhance the output. A PV cell can be electrically modeled as a current source in parallel to a diode, as shown in Figure 2.8. Two common parameters that characterize a PV cell are: open-circuit voltage and short-circuit current.

Typically, a PV cell can generate voltage between the range of 0.5 to 0.8 volts [29]. This is mainly dependent on the semiconductor used in the cell and the technology associated with it. It is noted that this voltage maybe very low, but this can be enhanced by connecting several cells in series or parallel to form a larger panel.

The semiconductors can mainly be broken down into three categories: monocrystalline, polycrystalline, and thin film. It is reported that monocrystalline have an efficiency between 10 and 15 percent, 9 and 12 percent for polycrystalline, and 10 and 12 percent for a thin film [30].

PV systems are reliable and friendly to the environment. The cell efficiency has improved, reaching for the most advanced laboratory cells of crystalline Silicon, to more than 24 percent, while commercial crystalline (silicon PV modules) are made of cells with efficiency in the range of 11 to 20 percent. The large introduction of PV systems may replace or postpone

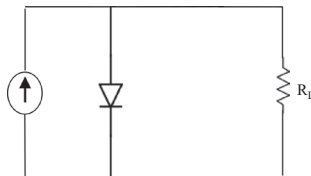


**Figure 2.8.** Circuit diagram of a PV cell.

the extension of conventional central stations of electricity production and the investment in grid reinforcement having a positive overall economic impact. The PV system electric power is of particular value when it coincides with the peak demand, as during the summer afternoon peak due to the use of air conditioning units. Moreover, PV systems could also contribute to the improvement in power quality, the reduction of electricity transport losses by producing at the point of consumption, and the increase of reliability of such systems [31].

## 2.6 COMBINED ENERGY HARVESTING

### 2.6.1 REVIEW AND BACKGROUND

Development of clean renewable energy technologies has received growing attention due to concerns about environmental damage and global warming. Scientists have researched and developed many ideas integrating solar PV and thermoelectric technologies [32, 33]. The designs have consisted of converting solar energy into electricity and usable heat at the same time.

A detailed review was conducted by Zondag [34] on photovoltaic–thermal (PVT) systems. The review has focused on ground grid-connected applications such as building-integrated designs, which have a lot of future potential. Conventional techniques such as gluing and laminating PV cells have demonstrated many drawbacks, including insufficient electrical insulation, large losses, and lack of sufficient protection from environment (such as moisture). One of the advanced techniques being used for more commercial PVT devices is by laminating the top cover, PV cells, insulation, and absorber in one step. The other advance technique used is the encapsulation. The outcome of this review paper also describes the thermal module efficiency in great deal, and it can be summarized as dependent on reflection losses, thermal resistance, and thermal losses. The PVT technology can be further classed as PVT liquid and PVT air.

Research carried out by Dupeyrat [35] is a detailed analysis of thermal and optical properties to achieve maximum efficiency by integrating PV and solar thermal functions. This research presented a theoretical background of a PVT collector having a combination of components of PV and thermal. Collectors can simultaneously cover demand of electricity and heat at the same location, hence demonstrating promising applications. A device was constructed using PV cells and integrated into a domestic hot water system, using water as a heat transfer medium. The device also incorporated a unique method of encapsulation different to other

conventional ways. Various experiments were conducted on this device and demonstrated varied characteristics of different materials. For the hot water system, the thermal efficiency was calculated between the ranges of 50 and 80 percent, whereas the electrical efficiency was noted at 8.5 percent. The results confirmed that, in hybrid mode, the thermal efficiency was much lower than pure thermal mode as a result of converting part of the solar radiation into electricity. An increase of  $2\text{mA}/\text{cm}^2$  in generated current density was seen with the new structure and process of encapsulation. These results presented much favorable performance characteristics in comparison to other PVT collector concepts and devices.

A solar-driven hybrid system combining solar cells and TEGs was developed by Deng [36]. The overall design consists of silicon solar cell, TEG, and a heat collector to achieve high power generation. A bowl-shaped heat collector with an absorbing, conducting, and insulation layer is added to the system. A copper coil is used to conduct heat to TEG to produce electricity. Several simulation and experimental tests were carried out mostly using the illumination intensity of  $60\text{mW}/\text{cm}^2$ . The commercial software ANSYS was used to produce thermoelectric analysis. The study also conducted a cost analysis by comparing the cost per watt-peak of power generated of solar cells and TEG on their own. The study concluded enhanced power generation of around  $393\text{mW}$ , which is twice the amount generated by solar cells alone. Much more heat was collected on the hot side of TEG due the design of the collector.

Liao [37] constructed a hybrid device consisting of low-concentration PV module and a semiconductor TEG. The performance of the device is dependent on thermodynamic and thermoelectric parameters. These are predominantly defined as working temperature, current, optical concentration ratio, figure of merit, and thermal conductance. A series of equations is derived for the performance of the hybrid device and experimental data is gathered. This study shows the general performance characteristics, and the optimum criteria of parameters are derived. The study concluded with promising results of higher power output and efficiency of the hybrid results than conventional PV devices or TEGs on their own.

Khasee [38] carried out analysis of energy and exergy for a thermoelectric solar air collector device. Several conclusions of the study were drawn regarding the performance, efficiency, and future developments in the technology. It proposed that the energy efficiency is higher than that of the exergy efficiency of the thermoelectric solar collector. Experimental data concluded that, by increasing the air flow rate, the thermal exergy efficiency increases; the reported efficiencies found were 80.3 and 8.4 percent, respectively.

### 2.6.2 FUTURE TRENDS AND COMMERCIAL PATENTS

In spite of an ever-growing interest in the field of integrating PV modules and TEG for co-generation of electricity and heat, no significant technological breakthrough has taken place for a highly efficient system that can be installed on rooftops. Researchers are constantly looking at alternative ways to reduce the heat losses, such as reflection losses, which result in reduction of usable heat. Another aspect that needs to be investigated is the reliability of the combined energy harvesting system. There are many issues reported, which will need to be looked at such as overheating, electric insulation, and safety.

Areas of future development identified by Khasee [38] refer to using a reflector to improve the thermal and electrical power output of the double-pass thermoelectric solar air collector.

A few patents exist within the area of PV and thermal panels to produce electricity. A patent submitted in 1986 by Jarnagin [39] relates to PV-solar heated panel. The design and way to mass produce PV surfaces continuously on copper substrate without growing or cutting conventional boules or mounting small pieces onto panels has been protected.

Solar thermal collectors have been made in the past in long strips, which can then be installed on top of the roofs. A patent by Ansley [40] was submitted in 2004 to protect their invention using a specific design and combining the technologies. An aspect of the invention is a flexible thermal solar collector and a PV device mounted on the thermal collector to become a solar power assembly.

## CHAPTER 3

---

# PIEZOELECTRICITY

### 3.1 BACKGROUND THEORY

The Currie brother's discovery only predicted direct piezoelectric effect. The French physicist, Gabriel Lippman, was able to derive the converse effect mathematically in 1881. Later, the discovery made by Lippman was endorsed by the Currie brother's in other published material.

A piezoelectric material produces an electric charge when the substance undergoes mechanical stress. To explain this effect, we look at the molecules that make up the crystal as adapted in Figure 3.1 [41]. Each molecule is polarized, where one end is more negatively charged and the other end is positively charged. In a monocrystal, the polar axes of all of the dipoles lie in one direction. Whereas, in a polycrystal, there are different regions with different polar axes. A monocrystal is symmetrical, and a polycrystal is asymmetrical. If we cut the polycrystal, the two remaining pieces will not have the same resultant polar axis.

In order to harvest the piezoelectric effect, the polycrystal is heated up using a strong electric field. Molecules get heated up due to the electric field which then forces the dipole to align almost in the same direction.

To explore this further, when force is applied to the piezoelectric material or it is compressed or stretched, this develops a voltage. The voltages developed by compressing and stretching have opposite polarity. Conversely, if we apply voltage across the piezoelectric material, with the same polarity, we will see a deformation in the material (expansion). However, if we reverse the polarity of voltage, the material will compress.

The amount of energy stored in a piezoelectric element is the same as the energy stored in a capacitor [42]:

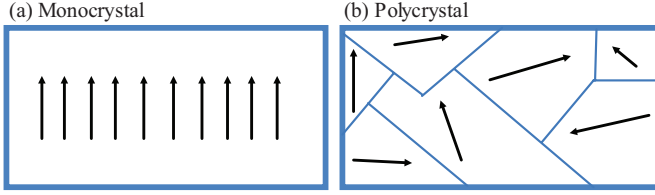


**Figure 3.1.** Structure of piezo crystals.

$$E_C = \frac{1}{2} CV^2 \quad (3.1)$$

where  $C$  is the capacitance and  $V$  is the voltage produced.

We can use two types of signals for such generators: direct piezoelectric effect and converse effect, as described earlier in the chapter. Direct piezoelectric effect can be described as conversion of mechanical into electrical signals mostly used in sensors. The converse effect can be explained as electrical sollicitation into mechanical energy and mostly used for actuators.

The generated charge density is [18]:

$$D = \frac{Q}{A} = d_{3n} F_n \quad (3.2)$$

where  $D$  is surface charge density,  $Q$  is the charge developed,  $A$  is the conductive electrode area,  $d_{3n}$  is the piezoelectric co-efficient for the axis on which stress or strain is applied, and  $F_n$  is the force applied in relevant direction.

The EMF is defined as [18]:

$$emf = g_{3n} F_n t \quad (3.3)$$

For both equations 3.2 and 3.3;  $n$  is defined as the direction of axis for stress and is denoted by 1, 2, or 3 (where 1 represents the length direction, 2 represents the width direction, and 3 represents the thickness direction).

## 3.2 PIEZOELECTRIC MATERIALS

Piezoelectric materials can be used to harvest energy by simple conversion of oscillatory energy into electrical energy. Combining this technology with mechanical coupling designs, we can harvest energy from

mechanical motion. This scheme offers various advantages for powering small-scale systems that are powered by clean sources of energy.

There are many materials such as quartz and tourmaline crystals that exhibit piezoelectric effect. These materials have, in the past, been actively used as electromechanical transducers [43]. Another group of materials (ferroelectric materials) that exhibit piezoelectric effect are known as piezoelectric ceramics. Table 3.1 shows the piezoelectric constants as experimentally calculated by other researchers [44, 45]:

### 3.2.1 FERROELECTRIC CERAMICS

Ferroelectric ceramics are an important group of the piezoelectric materials. They can be used as resonators, bandpass filters, discriminators, surface acoustic wave (SAW) filters, and have various other applications. Ceramics such as lead zirconate titanate (PZT) are widely used in energy harvesting due to its favorable properties. In each PZT crystal, the positive and negative charges are separated and distributed in the array symmetrically. This ensures that under normal conditions, PZT is neutral. By applying any kind of force or stress to the material, this symmetry is disturbed, resulting in a voltage drop across the material.

PZT is considered to be a prospective replacement for batteries because of high piezoelectricity and energy density. PZT is often used in a specific composition to achieve a particular crystal structure and the desired piezoelectric effect. PZT is an oxide alloy of lead, zirconium, and titanium and is one of the most researched and viable inorganic piezoelectric ceramic to achieve the desired effect [46]. PZT has a rigid lattice, which allows the positive ions to move within the structure. Experimental studies [47, 48] have shown that increasing the temperature increases the dielectric constant of PZT. Young's modulus of PZT is also dependent on temperature.

There are many factors that affect the power consumption and life of a piezoelectric device. In conditions of high humidity, leakage current

**Table 3.1.** Materials with piezoelectric constant

Material	Piezoelectric constant $\times 10^{-12}$ m/V
Quartz	2.3
Barium titanate	100–149
Lead niobate	80–85
Lead zirconate titanate	250–365

increases the power consumption of devices. This can lead to the device failing, but studies have shown no change in piezoelectric properties [49].

PZT has many applications in harvesting energy. One of the applications was developed by Howells, Heel-Strike System for military and commercial use [50]. The system consisted of two pieces, the heel-strike generator, and power electronics circuit. The purpose was to convert the unusable power from the heel-strike generator to something more useful. The mechanical energy would be transferred into electrical energy. The system was then tested at various compressions to evaluate the output energy. On average, it was noted that 0.0903 W per compression was produced. Although the desired outcome of power was much less than anticipated as several issues were found during the development of this project. If the issues highlighted in the study are addressed, the heel-strike generator should be able to produce more energy.

### 3.2.2 ORGANIC MATERIALS

For future electronic applications, substrate and piezoelectric materials are required with properties of wide degree of freedom in shapes with flexible, transparent, and stretchable characteristics. They will certainly position themselves in various applications even beyond mobile or handheld devices, for example patch-type health care devices and wearable energy-generating sources for flexible electronics. A ZnO nanowire-based piezoelectric generator is used for microsystem application. However, these inorganic-based structures have the constraint of low flexibility and low piezoelectric property. Researchers are now focusing on new organic-based piezoelectric materials.

In joint research of Murata Manufacturing Co Ltd, Kansai University and Mitsui Chemicals Inc. [51] have developed a new organic material. It is made of special polyester and used in two prototype devices: leaf grip remote controller and a touch pressure pad. This technology fulfills the demand for a new human-machine interface (HMI). It further increases the usability of smart phones and other devices. The prototypes are undergoing testing before they would be commercially available.

### 3.2.3 FUTURE PROSPECTS

So far, we have established that the power output for piezoelectric and thermoelectric is much lower than photovoltaic. Photovoltaics are also dependent on light intensity and will not be able to deliver the maximum output all the time. The power output is dependent on many factors that

have been discussed in the previous topics. Ideally, we want to support devices that have higher power consumption and require power continuously. Relying on just one energy source will limit the use of such energy harvesting techniques. One solution is to develop a hybrid system or combine two or three energy harvesting technologies.

One study was conducted on combining thermoelectric generators, pyroelectric generator, and piezoelectric materials [52]. The system was able to generate electricity using two different energy conversion principles: pyroelectric effect and piezoelectric effect. The two energy conversion methods were used simultaneously, thereby giving a higher output. The design features included ensuring the induced voltage of the same sign for both conversion techniques; otherwise, it risked canceling each other. The rather low efficiency of pyroelectric generators was enhanced using the combined energy harvesting technique.

The photovoltaic and thermoelectric devices have been researched by several groups [53, 54, 55]. Another study looked at integrating solar cells and thermoelectric devices and designing a hybrid energy harvesting system [56]. By integrating a thermoelectric device with the photovoltaic modules, the output was increased dramatically. The study recorded current density and voltage curves and concluded maximum power in the range of 9 to 11 mW/cm<sup>2</sup> at a temperature gradient between 5°C and 9°C.



# PIEZOELECTRIC ENERGY HARVESTING TECHNIQUES

## 4.1 MODELING

In order to model a piezoelectric energy harvester we need to understand the piezoelectric effect and strain–charge relationships using the derived equations [57]:

$$S = [s^E]T + [d^t]E \quad (4.1)$$

$$D = [d]T + [\epsilon^T]E \quad (4.2)$$

where  $D$  is electric displacement of charge,  $E$  is the electric field strength,  $S$  is the mechanical strain,  $T$  is the mechanical stress,  $\epsilon^T$  is permittivity of material under constant stress and  $s^E$  is the compliance under a constant electrical field,  $d$  is the matrix for direct piezoelectric effect,  $d^t$  is the matrix for reverse piezoelectric effect and  $t$  denotes the matrix transposition. Thus, equations 4.1 and 4.2 represents direct and reverse piezoelectric effect, respectively.

$E$  and  $D$  are defined as electrical quantities with vector nature, whereas  $T$  and  $S$  are mechanical quantities with tensor nature of six components. The constants in a piezoelectric material referred as  $d$ ,  $\epsilon$ , and  $e$  depend on the directions of electrical field, displacement, and stress and strain, respectively.

In three dimensions, the piezoelectric effect is given by [57]:

$$\begin{pmatrix} D_1 \\ D_2 \\ D_3 \end{pmatrix} = \begin{pmatrix} 0 & 0 & 0 & 0 & d_{15} & 0 \\ 0 & 0 & 0 & d_{24} & 0 & 0 \\ d_{31} & d_{32} & d_{32} & 0 & 0 & 0 \end{pmatrix} + \begin{pmatrix} T_1 \\ T_2 \\ T_3 \\ T_4 \\ T_5 \\ T_6 \end{pmatrix} \begin{pmatrix} \varepsilon_{11} & 0 & 0 \\ 0 & \varepsilon_{22} & 0 \\ 0 & 0 & \varepsilon_{33} \end{pmatrix} \begin{pmatrix} E_1 \\ E_2 \\ E_3 \end{pmatrix} \quad (4.3)$$

For direct piezoelectric effect, we use Equation 4.1 to deduce the following co-efficient:

$$d_{ij} = \left( \frac{\partial D_i}{\partial T_j} \right) E = \left( \frac{\partial S_i}{\partial E_j} \right) T \quad (4.4)$$

$$e_{ij} = \left( \frac{\partial D_i}{\partial S_j} \right) E = \left( \frac{\partial T_i}{\partial E_j} \right) S \quad (4.5)$$

The energy stored in a piezoelectric material is modeled as energy stored in a capacitor. Thus, the following equation is derived:

$$W_{33} = \frac{1}{2} Q_{33} V_{33} \quad (4.6)$$

Where  $Q_{33}$  and  $V_{33}$  are described as:

$$Q_{33} = d_{33} F_3 \quad (4.7)$$

$$V_{33} = \frac{T}{WL} F_3 g_{33} \quad (4.8)$$

where  $T$  is the thickness,  $W$  is the width,  $L$  is the length,  $F$  is the force applied, and  $g_{33}$  and  $d_{33}$  are constants related to the piezoelectric material used.

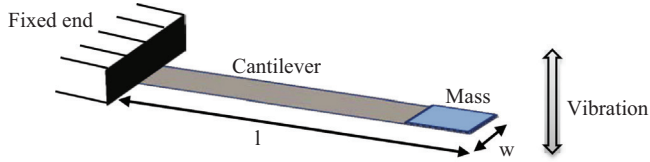


**Figure 4.1.** Cantilever arrangement with mass.

## 4.2 MECHANICAL AND ELECTRICAL BEHAVIOR

Most piezoelectric energy harvesting systems are based on a cantilever arrangement, as shown in Figure 4.1, and the focus of this book is on such an arrangement. In order to develop an electrical equivalent circuit, we will need to understand the electrical generation from mechanical energy by vibrations.

Resonant frequency of a spring-mass structure can be determined by:

$$f_r = \frac{1}{2\pi} \sqrt{\frac{k}{m}} \quad (4.9)$$

where  $k$  is the spring constant and  $m$  is the inertial mass.

For Figure 4.1, the resonant frequency with a mass at free end can be determined by [58]

$$f_r = \frac{1}{2\pi} \sqrt{\frac{Ywh^3}{4l^3 (m + 0.24m_c)}} \quad (4.10)$$

where  $Y$  is Young's modulus,  $w$ ,  $h$ , and  $l$  are the dimensions of the cantilever,  $m_c$  is the mass of the cantilever, and  $m$  is the mass at the free end.

Piezoelectric beams are generally a bimorph structure where a substrate layer is sandwiched between two piezoelectric layers. Figure 4.2 shows an equivalent circuit of a lead zirconate titanate (PZT) beam. In this circuit, the voltage source is connected in series with RLC and builds up a resonant circuit.

## 4.3 CIRCUIT TOPOLOGIES

A piezoelectric material produces alternating voltage and current from an alternating mechanical stimulus. In order to harvest energy from a piezoelectric material, we need to rectify the alternating output to direct

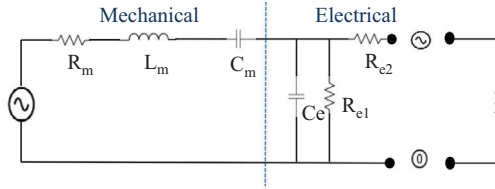


**Figure 4.2.** Equivalent circuit model for piezoelectric energy harvester.

output. This can be achieved in various ways. We will review two ways of rectifying the output:

#### 4.3.1 FULL-BRIDGE RECTIFIER

In vibrational energy harvesting, a full bridge rectifier is a common solution to the problem of alternating output. To create a full bridge rectifier, four diodes are connected in a Wheatstone bridge formation, smoothing the output. During the positive half-cycle, two diodes conduct in series, while the other two switch off; hence, the current flows through the resistive load. During the negative half-cycle, the other two diodes now conduct in series and other two switch off, ensuring current flows through the resistive load. This formation ensures the current flows in the same direction through the resistive load, hence smoothing the alternating output to direct output. We can further connect a capacitor that will smooth out the output, as shown in Figure 4.3.

#### 4.3.2 VOLTAGE DOUBLER

A voltage doubler as shown in Figure 4.4 produces twice the level of voltage as the input. It can take an AC voltage from a piezo device and convert it into a double DC voltage. This can be achieved by two diodes. On the negative half-cycle,  $C_2$  is charged to voltage  $V_{out}$ . On the positive half-cycle,  $C_1$  is charged to a voltage of  $V_{out}$  too. Hence, the capacitors are in series, the output voltage would be twice of  $V_{in}$ .

### 4.4 EXPERIMENTAL WORK

A device was fabricated by sandwiching the PZT material between two steel strips [59]. The material was then compressed by applying mass

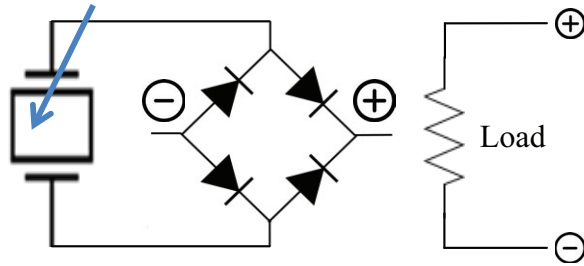


**Figure 4.3.** Full-wave bridge rectifier.

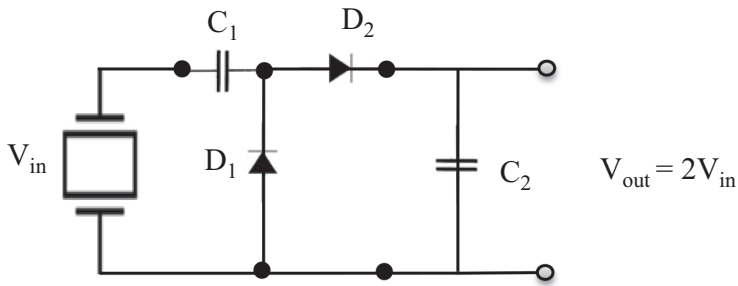


**Figure 4.4.** Full-bridge rectifier and voltage doubler connected to piezoelectric energy harvester.

in the range of 0 to 1,500 g. Two significant tests were carried out for open-circuit and resistive load. The maximum voltage harvested at the open circuit was 14 V. At resistive load, the maximum voltage harvested was between 6 and 9 V for 2.2 and 3.3 M $\Omega$ , respectively.

No load was connected across the PZT arrangement for linear compressions, and the voltage output was measured. The range of test facility was only between 0 and 1,500 g, which affected the maximum voltage harvested. The voltage is seen to drop just after the 1,500 g, as the test facility is unable to apply anymore force. Even though the voltage was seen to rise, the force sensor was unable to collect any good data; hence, any voltage harvested beyond 1,500 g was ignored in this study. Figure 4.5 shows the voltage versus mass at no load during the experimental stage.

Table 4.1 represents the data collected when harvested voltage was measured with resistive loads of 1, 2.2, and 3.3 M $\Omega$ . It was observed that the output voltage was higher during compression rather than de-compression. It was also observed that a maximum value of voltage at output was

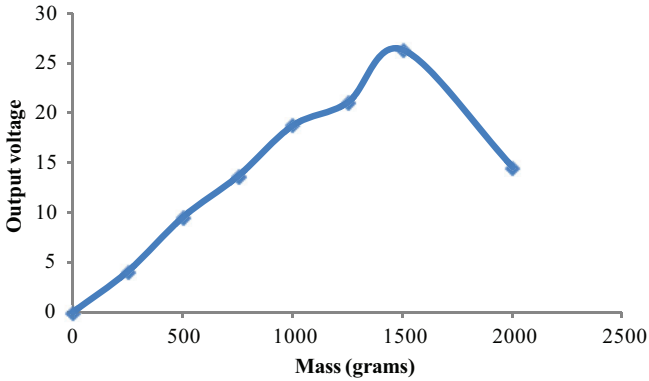


Figure 4.5. Mass versus output voltage at no load.

Table 4.1. Output voltage at various loads

Mass (grams)	1 M $\Omega$	Voltage (V) 2.2 M $\Omega$	3.3 M $\Omega$
250	0.33	0.49	1.11
500	0.63	1.22	2.89
750	0.89	2.89	4.85
1,000	1.20	3.33	6.21
1,250	2.11	4.29	7.87
1,500	2.80	6.90	9.40

seen at 1,500 g, which was the maximum mass or force applied onto the PZT material through the test facility. Using the trend, we can assume that the output voltage would increase further until the maximum power point was reached.

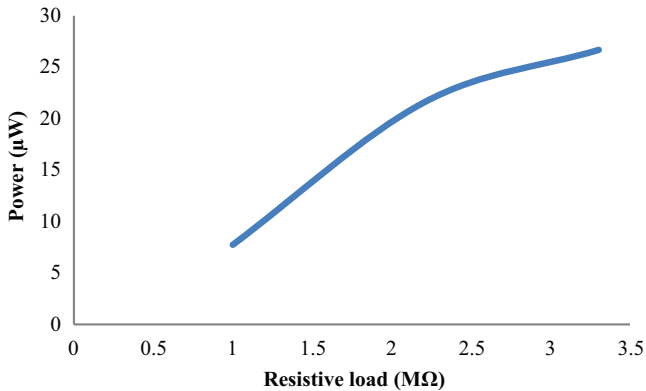
Tables 4.2 and 4.3 represent data collected for linear compressions and motion:

Table 4.2. Power parameters for compressions

Resistive load (M $\Omega$ )	Max. voltage output (V)	Current ( $\mu$ A)	Power ( $\mu$ W)
1.0 M $\Omega$	2.80	2.80	7.84
2.2 M $\Omega$	6.90	3.13	21.6
3.3 M $\Omega$	9.40	2.84	26.7

**Table 4.3.** Power parameters for linear motion

Resistive load (M $\Omega$ )	Max. voltage output (V)	Current ( $\mu$ A)	Power ( $\mu$ W)
1.0 M $\Omega$	1.80	1.80	3.24
2.2 M $\Omega$	2.36	1.10	2.53
3.3 M $\Omega$	3.56	1.07	3.84

**Figure 4.6.** Output power against resistive load.

We were expecting the power output of the device to be higher, in the microwatt range. Maximum power output was achieved at compression of 1,500 g of about 26.7  $\mu$ W at 2.84  $\mu$ A. We are able to power up the blood glucose meter at the sleep mode, which only requires 2  $\mu$ A. Figure 4.6 represents how the power output changed with various loads which resulted in a higher power output at high resistive load. At this mode, the device stores the date and time of the device. Every time a user is taking a blood glucose level reading, the reading is stamped with date and time. The piezoelectric device built in this study is able to power the sleep mode of the device.

The factors contributing to a lower power output are as follows:

- Fragility of PZT
- Limited range of the force sensor



# RAINDROP ENERGY HARVESTING

Energy harvesting (EH) from the impact of raindrops has been gaining significant research interest over recent years by a handful of groups, and the potential still has not been fully unlocked. It is this raindrop energy harvesting (REH) that is the focus of this study. Many geographical locations receive a moderate to heavy rainfall, which can then be utilized to generate electricity as an alternative method to conventional and other mainstream renewable techniques. Energy output using such a system is very low in comparison to other forms of renewable power generation, but may be sufficient to power electronic devices in specialist low-power applications, where replacing batteries is not a feasible option.

The energy output in REH devices depends on the mass of the droplet, the velocity, and the mechanism of impact at which it strikes the harvesting device. The radius of rain droplet can vary between 1 and 5 mm depending on the geographical location and type of rain.

## 5.1 REVIEW OF PUBLICATIONS

REH techniques using piezoelectric materials simply convert the impact energy and subsequent mechanical vibration of the device into an electricity supply. Most previous studies on piezoelectric energy harvesting have concentrated on machine, human, and other environmental sources of vibration. To date, a very limited number of studies have been conducted on EH from raindrop impacts.

One of the earliest studies conducted on REH [60] recommended the use of harvesting devices based on impact of raindrops. For remote areas and cities not connected to the grid system, the emphasis has been on

renewable energy, primarily in the form of solar systems. Solar systems are more effective during a sunny spell, but prove ineffective during monsoon season. Bangladesh, which routinely has around four months of monsoon season, could find the implementation of an REH system to be very beneficial. The study also contributes a detailed rain pattern in Bangladesh and a positive energy output of various EH techniques, depending on the impact velocity and drop size.

One of the most significant studies carried out on REH [61, 62] in which the authors conducted extensive research on theoretical and experimental models. The piezoelectric material selected for the study was polyvinylidene fluoride (PVDF) given its favorable lightness, flexibility, and environmentally friendly properties. The theoretical study estimated the energy that could be harnessed during the impact of a raindrop. To reduce the weight and increase the efficiency, a single sheet of PVDF was used, rather than the combination of two sheets. A mechanical–electrical transient model was developed to predict the behavior of a piezoelectric cable device. The experimental phase of the project focuses on impact simulation of a piezoelectric sheet. By using the mechanical–electrical model, the authors were able to achieve conclusive results on the energy harvested. By using various drop heights and drop sizes, 1 nJ of electrical energy and 1  $\mu$ W of instantaneous power was harnessed as a minimum. By artificially creating a downpour, the energy harnessed was 25  $\mu$ J with a power output of 12 mW.

Another study [63] looked at harvesting energy from rainfall using commercial transducers. Experiments were conducted on the two materials Lead zirconate titanate (PZT) and PVDF as a means of drawing a beneficial comparison. The transducers were exposed under rain to determine the voltage levels generated by the impact of rain droplets. The study recommended the use of PVDF transducers for REH devices because they generate high power, have a lower cost, and are not toxic when compared with PZT transducers.

Another study [64] focused on a device with a combination of cantilevers and diaphragm structures forming the REH. A comparison of empirical and simulation data was presented. The prototype developed for the energy harvester consisted of several layers namely: silicon, polyamide, aluminum (Al), and the PVDF active layer. The focus in this research was on a meshed model of the harvester. The results show a displacement pattern for the center of the diaphragm with various thicknesses of Al and PVDF. To achieve optimum results, thinner Al and PVDF are used, as thickness is inversely proportional to maximum displacement. On the cantilever surface, as the thickness of PVDF is increased, the maximum

displacement begins to decrease, whereas the AI is directly proportional to the maximum displacement. It is concluded that PVDF thickness of 150  $\mu\text{m}$  and AI thickness of 35  $\mu\text{m}$  results in a maximum displacement of 2,800  $\mu\text{m}$ . However, at these thicknesses, the maximum displacement on the center of the diaphragm is relatively small. These thicknesses are able to withstand the impact pressure of a large droplet of 13.718 MPa. The maximum displacement limit is found to be 2,800  $\mu\text{m}$ .

A review [65] looked at the limited studies conducted on PZT and PVDF harvesters using droplet impulses. The study also included a comparison of the results obtained from a bridge and cantilever structure using a PVDF film. The experimental results illustrated that the cantilever structure only produces a few millivolts, as the structure is soft and easily deformed, whereas the bridge structure produced a higher voltage. The design of the bridge structure was supported at both ends, thus rendering it more rigid. The maximum voltage produced in the bridge structure was around 3.502 V, whereas the cantilever structure registered a corresponding maximum figure of 1.003 V. It was also observed that droplets pass through the cantilever structure and splash on the ground, whereas on the bridge structure, the droplets impact and splash on the beam, thereby absorbing more energy.

One of the most recent studies conducted by Nayan et al. [66] showcased the need of developing a rain harvester due to the favorable rainy condition in particular countries. The research focused on series- and parallel-connected devices and proposed a design for the piezoelectric plate. The output of the piezoelectric device was found to be dependent on the impact pressure on the piezoelectric body. The voltage output was measured for different droplet heights, and simulations were carried out for different design approaches.

Another study [67] compared PVDF and PZT materials. The devices with these materials were exposed under rain to determine the voltage levels generated by the impacts. The study recommended the use of PVDF devices for REH because they showed these generated higher power output.

A theoretical review [68] focused on the proposal of the idea of a *Piezoelectric Shingle* as a new EH system, based on meteorological precipitations as the rain. It presented a preliminary analysis about the state of art of EH systems, based on piezoelectric technology, showing potentiality, limits, and other experiences in the field of interest. It reviews the main features of rainy phenomena, interesting for an EH system, reconsidering some theoretical or empirical models. Models are addressed to define the limit velocity of raindrops and a distribution law between

dimension of raindrops and the nature of rainfall. After considerations about the annual quantity of water fallen in a region, the authors propose the ideation of some key patterns for a piezoelectric EH system from rainy precipitations.

Maximum power output using a water vortex [69] on a macrofiber composite piezoelectric energy harvester was found to be around  $1.32 \mu\text{W}$  with a water velocity of  $0.5 \text{ m/s}$  at the cylindrical diameter of  $30 \text{ mm}$ . By using an upright vortex-induced piezoelectric energy harvester [70], the power output was found to be  $84.49 \mu\text{W}$  using a velocity of  $0.35 \text{ m/s}$ .

## 5.2 CHARACTERISTICS OF A HARVESTER

### 5.2.1 IMPACT VELOCITY

A raindrop in freefall toward the ground experiences two forces that are exerted vertically on it: a force acting upward, known as the drag force, and the force acting downward, the gravitational force resulting in the weight of the droplet.

The drag force on the droplet is represented in Equation 5.1, where  $\rho_a$  is the density of air,  $A$  is the projected frontal area of the droplet,  $v$  is the velocity of the droplet, and  $C$  is the coefficient of drag.

$$F_{air} = \frac{1}{2} \rho_a A C v^2 \quad (5.1)$$

The weight of the droplet is represented in Equation 5.2, where  $\rho_w$  is the density of the water droplet,  $r$  is the radius of the droplet, and  $g$  is the acceleration of the droplet due to gravity.

$$F_{gravity} = \frac{4}{3} \pi r^3 \rho_w g \quad (5.2)$$

When these forces are in balance, the droplet reaches its terminal velocity,  $v_T$ , the maximum velocity if no other forces act on the raindrop. This is shown in Equation 5.3, where  $d$  is the diameter of the droplet.

$$v_T = \sqrt{\frac{\pi d^3 \rho_w g}{6 \rho_a A C}} \quad (5.3)$$

### 5.2.2 IMPACT MECHANISM

The impact mechanism will significantly influence the energy transfer function of the harvesting device and its power output. Generally, the impact mechanism of a droplet falling onto a solid surface can be divided into three main categories: (1) bouncing, (2) spreading, and (3) splashing. The water droplet can either fully bounce leaving no water residue on the solid surface, which is depicted in Figure 5.1(a), or partially bounce leaving water residue, as depicted in Figure 5.1(b). The second category of the water droplet is spreading on impact, when the water adheres to the surface at impact, as depicted in Figure 5.1(c). The third category of the water droplet is splashing, when the droplet breaks into many parts and adheres to the surface. The droplet will then be distributed on the surface as depicted in Figure 5.1(d). The impact of a droplet on a harvesting device is expected to demonstrate all or a combination of these mechanisms. Studies have shown these types of droplet impact mechanisms on solid surfaces [71, 72].

Various studies show the dominant impact mechanism of a water droplet is one that involves splashing [73]. An empirical relation, as represented in Equation 5.4, is developed by Stow et al. [74] and by Mundo et al. [75] from experiments, where  $R_e$  is the Reynolds number (a dimensionless number defined as the ratio of inertial forces to viscous forces),  $W_e$  is the Weber number (a dimensionless number with relative importance of fluids inertia compared to surface tension), and  $K$  is defined as a constant (which depends on the roughness of solid surface and thickness of layer).

$$K = W_e^{\frac{1}{2}} \times R_e^{\frac{1}{4}} \quad (5.4)$$

The Reynolds and Webber numbers are found from the following equation where  $\rho$  is the density of fluid,  $\mu_a$  is the viscosity,  $\sigma$  is the surface tension of the fluid, and  $v$  is the velocity:

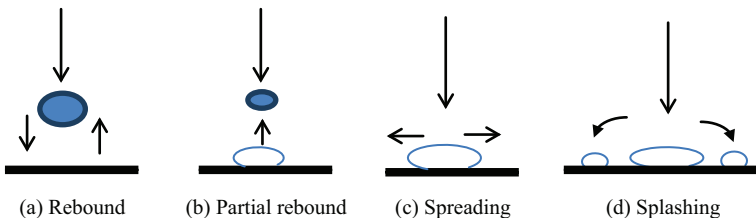


**Figure 5.1.** Water droplet impact on solid surface.

$$R_e = \frac{\rho_w v d}{\mu_a}; W_e = \frac{\rho_w v d}{\sigma} \quad (5.5)$$

It was proposed that the behavior of the water droplet can be determined by Equation 5.5, which will either deposit on the surface or splash. If  $K$  is found to be smaller than a particular  $K_c$ , a threshold value, then only deposition will occur, and if  $K$  is greater than this  $K_c$  then a splash will develop [76].

A study of the impact of a water droplet should also consider whether the impacted surface is horizontal or inclined. Investigations conducted by Sikalo et al. [77] analyze the theoretical and experimental results of horizontal and inclined surfaces. The effect on horizontal surface was found to be mainly due to surface material properties, impact velocity, droplet viscosity, droplet surface tension, and droplet size. The surface of impact plays an important role where the maximum spread is large on a glass surface in comparison to wax and polyvinyl chloride (PVC). The maximum spread and spreading velocity increase with increasing the impact velocity. Water, isopropanol, and glycerin droplets are used in the experiments with nearly the same Weber and Reynolds numbers. The results of the experimental study formulated the empirical model of impacting droplet–surface interaction. The maximum spread increases with increasing the Reynolds and Weber numbers. Another study [78] reviewed the impact onto an inclined surface, which was dependent on droplet material properties such as viscosity, density, and surface tension. The rebound effect could only be achieved on a dry smooth glass and on wetted surfaces. There was no rebound on wax and rough glass. It was concluded that the temperature of droplet and surface has no significance on the bouncing or spreading of droplets.

The objective of this study was to investigate the conversion of water droplet kinetic energy using a piezoelectric EH (PEH) device to convert the impact and vibrational energy of the device into electrical energy. As the droplet fell from standstill, it accelerated along a path increasing in velocity. As discussed previously, the droplet can reach equilibrium at a certain stage, as represented by Equation 4.5. The kinetic energy of the droplet is then related to the velocity and droplet size, as shown in Equation 5.6.

$$E_{KE} = \frac{1}{2} \rho_w \left( \frac{4}{3} \pi \left( \frac{d}{2} \right)^3 \right) v^2 \quad (5.6)$$

The droplet harvester is not expected to be able to extract all this energy, even if it is an optimized harvester; however, a Betz type limit is expected to apply as deposits on the harvester need energy to be removed.

### 5.2.3 SURFACE INTERACTION

Rain and other forms of precipitation occur when warm moist air cools and condenses. This happens as a result of moisture condensing to liquid, as warm air can hold more water than cool air. Also, rain can be categorized into convection or stratiform. The cycle of convection mostly occurs in regions closer to the equator where the moisture in the ground is heated above the temperature of the surrounding areas, leading to an increase in evaporation. As the water vapor rises, this condenses into clouds, which then subsequently can produce rain. The resulting convective shower mostly occurs for a short period of time over a limited area. Areas surrounding the equator are most likely to receive regular convective showers. For example, in the United Kingdom, this phenomenon is referred to as *sunshine and showers* as it rains in a smaller area followed by clear spells. This type of rain mostly occurs in the South and East of the United Kingdom.

Stratiform rain occurs when warm and cold air meet, but do not mix easily because they have different densities. Normally, under these conditions, the warm air rises over the cold air creating a *front*. When air is forced up a mountainside, the water vapor in that air then condenses and falls as raindrops. Generally, warm fronts are followed by light showers. The duration of stratiform rainfall is less, but the intensity can be high [79].

Stratiform rain is further categorized into three types: light stratiform rain (LSR), moderate stratiform rain (MSR), and heavy thunderstorms (HT). Some typical values of raindrop size and velocity measured by Perera [73] are presented in Table 5.1.

The fluid mechanics of droplet impact with a surface is of importance in a variety of different fields. The fluid flow associated with impinging drops is nontrivial and not fully described in detail in the scientific literature. A raindrop impact on a liquid surface can splash or bounce, as well as merge with any surface liquid, whereas a raindrop impact on a solid surface will either splash or spread out on the surface. The phenomenon is discussed in more detail in an earlier publication [80].

Another feature to take into consideration is that the harvester surface can generally be either smooth or rough. It is reported [81] that splashing

**Table 5.1.** Raindrop size versus terminal velocity (Taken from [80])

Rain type	Drop size (mm)	Terminal velocity (m/s)
<i>LSR</i>		
Small	0.5	2.06
Large	2.0	6.49
<i>MSR</i>		
Small	1.0	4.03
Large	2.6	7.57
<i>HT</i>		
Small	1.2	4.64
Large	4.0	8.83
Largest	5.0	9.09

is reduced when highly polished surface is used. In many problems, the elastic response of the surface is insignificant. However, the elasticity of the surface can no longer be neglected when high-speed drops collide with a surface.

During the initial stage of impact, the drop is merely deformed and compressed at its base. Hence, surface tension forces and the viscosity of the liquid do not enter the scenario at this stage. The important parameters are density and compressibility of the liquid, and the impact velocity and diameter of the drop. In the contact zone between the drop and the surface, pressure is not uniform.

Splashing is a phenomenon often observed during liquid droplet impact onto a solid surface. The threshold of splashing is known to be related to droplet size, impact velocity, and physical properties of the liquid, but the mechanisms that initiate splashing are not understood completely. In accordance with the Kelvin–Helmholtz (K–H) instability analysis, recent studies [82] have shown that ambient gas density has a significant effect on the threshold and trajectory of splashing. Research has focused on the effects of droplet velocity, impact angle, and ambient gas pressure (or density) on the threshold of splashing, and the motion of the ambient gas surrounding the droplet was examined. Experimental observations of splashing were carried out with a droplet of 1.7 mm in diameter, while varying droplet velocity, impact angle, and ambient pressure. An empirical correlation was derived using our and other published data to determine the threshold of splashing based on the aforementioned parameters. Also, a numerical simulation using the volume of

fluid method was carried out to calculate the gas velocities surrounding the droplet during impact. The results of this model gave supportive evidence that K–H instability is a suitable instability theory that helps explain the splash phenomenon, with consideration of the gas motion surrounding the droplet.

## 5.3 EXPERIMENTAL INVESTIGATION

Ilyas and Swingler [83] conducted an in-depth study of a PEH using the impact of raindrops. The experimental setup was done in a cantilever style. The research focused on understanding how the device behaves and which parameter were associated with the harvested power. This chapter will further explore the findings from their study.

### 5.3.1 VOLTAGE PROFILE

The device used was a commercially available piezoelectric sensor with PVDF as the active material. Experiments were divided into three regions as to where the water droplets would impact the device, as shown in Figure 5.2.

Before the water droplet impacts the device, the piezo sensor is at a horizontal position close to the zero position. As the water droplet falls onto the sensor, it interacts with the sensor and starts to push the sensor downwards from position 1 *Droplet impact start sequence* to position 2 *Maximum negative velocity of device sensor*. The sensor accelerates during this time and reaches a maximum negative velocity at position 2, resulting in a maximum negative voltage. The sensor then decelerates and reaches its full deflection at position 3 *Full deflection of device sensor*, resulting in a zero voltage. The device sensor then starts to rebound and accelerate back in the opposite direction and reaches its maximum positive velocity at position 4 *Maximum positive velocity of device sensor*. This results in a maximum positive voltage output, which is the maximum voltage

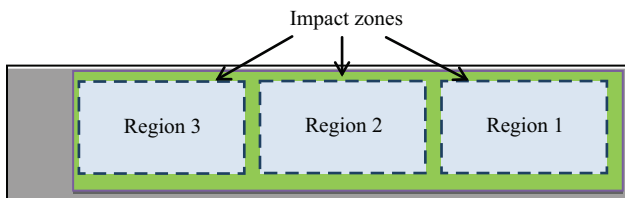


**Figure 5.2.** Impact zones for water droplets on a piezo device.

magnitude of the whole event. After this point in the whole event, the voltage output oscillations and deflection oscillations of the sensor decay away. As was expected, the first deflection of the sensor in the negative position when pushed down by the droplet impact was the largest maxima of all subsequent maxima of the oscillations. It should be noted that the droplet does not deliver all its energy at the first instant of the impact, but takes a finite time as the droplet interacts with the device sensor. The impact mechanism is complete and available energy fully delivered when the full deflection of the device sensor is reached at position 3. Figure 5.3 shows the device sensor deflection position (which is derived from the voltage output). [80].

Figure 5.4(a) depicts the voltage output profile of a single EH unit of a water droplet impact event [80]. An oscillating profile is shown, which consists of two stages as the event evolves with time. These stages are shown

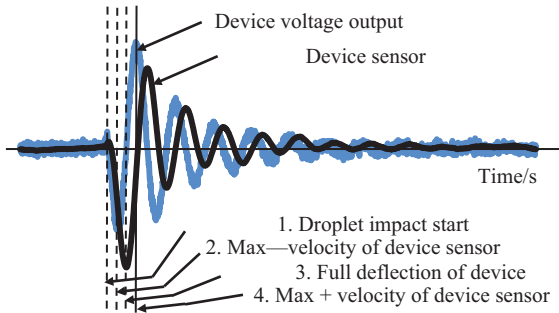


**Figure 5.3.** Voltage output and sensor position profiles of the device (Taken from [80]).

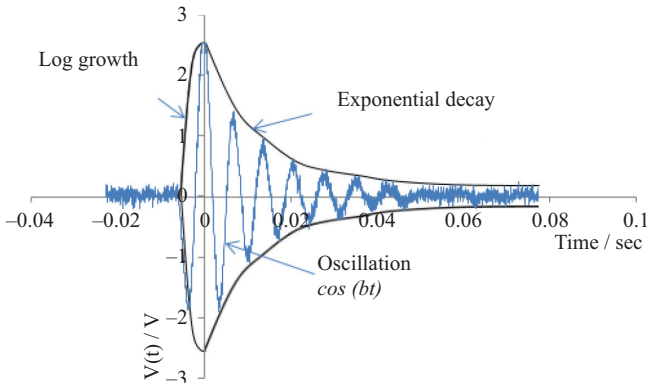


**Figure 5.4.** Voltage output of harvester for an impact (Taken from [80]).

in Figure 5.4(b) as the *log growth* stage as the voltage grows to a maximum followed by the *exponential decay*, stage as the voltage decreases to zero.

The oscillating profile is of a cosine form, which is seen in the two stages. The log growth stage in the voltage consists of a growth term and the cosine term, as shown in Equation 5.7, where  $V_{Peak}$  is the highest voltage attained, and  $t_p$ ,  $c$ , and  $e$  are constants:

$$V(t) = \left( \frac{2V_{Peak}}{1 + \exp(c(t - t_d))} - V_{Peak} \right) \cos(et) \quad (5.7)$$

The exponential decay stage of the voltage consists of a decay term and the cosine term as shown in Equation 5.8, where  $a$  is related to the half-life of decay,  $t_{1/2}$  and  $b$  are related to oscillation frequency  $f$ , as shown in Equation 5.9:

$$V(t) = V_{Peak} \exp(-at) \cos(bt) \quad (5.8)$$

$$V(t) = V_{Peak} \exp\left(-\frac{\ln(2)}{t_{1/2}}t\right) \cos(2\pi ft) \quad (5.9)$$

### 5.3.2 SINGLE DEVICE

Initially, voltage against load was experimentally calculated, as shown in Figure 5.5, which was broken down by different heights. It can be

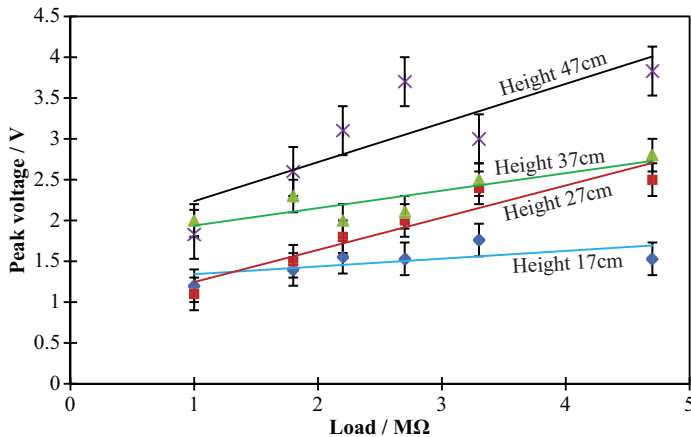


**Figure 5.5.** Voltage against load for a single device (Taken from [80]).

seen, as the height increases, this has a direct impact on the peak voltage obtained. [80].

Experiments were then conducted against different angles to deduce the best region and angle to drive maximum output. As the angle of the device is increased from  $0^\circ$  to  $45^\circ$ , it was observed that the peak voltage decreases. This can be due to the impact position of the droplet. When the device is at  $0^\circ$ , the droplet normally splashes on the device and most of it is retained on the surface of the device, hence giving a higher output. When the droplet impacts the device at an angle, most of it disperses and bounces off the device; hence, a lower output is observed. The peak power attained was in the region of 4 to 18  $\mu\text{W}$ , as shown in Figure 5.6.

### 5.3.3 MULTIPLE DEVICES

Further experiments were conducted on a module of multiple devices, which was then repeated both for rectified and non-rectified versions. The non-rectified module shows a significant decline in the energy output as more devices are added in parallel in the module. The energy output of the module (with multiple devices) is shown in Figure 5.7. [83]

### 5.3.4 EFFICIENCY OF THE DEVICE

Using the simplified equivalent circuit (as demonstrated in Chapter 4), the voltage equation is developed. The voltage drop across the source and

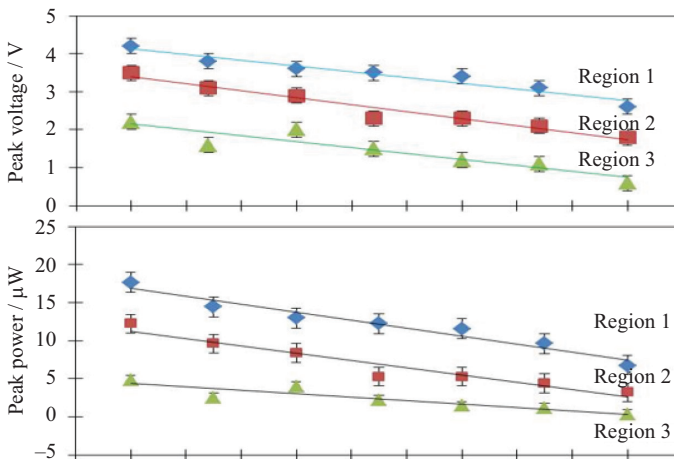
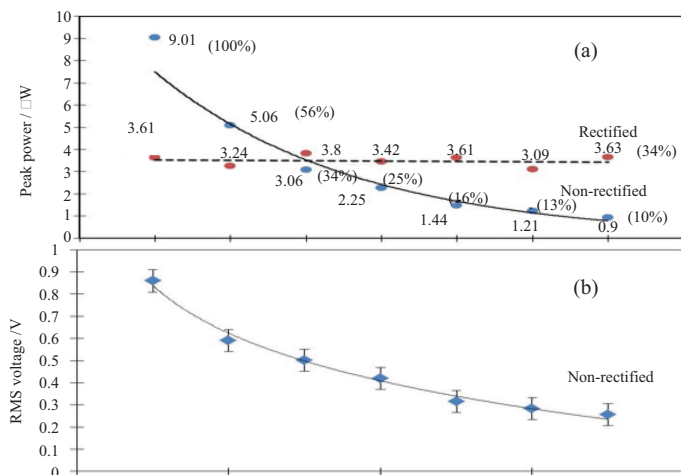


Figure 5.6. Voltage and power profiles of a single device (Taken from [80]).



**Figure 5.7.** Voltage and peak power the module with multiple devices (Taken from [83]).

load is given by Equation 5.10; the voltage of the simplified theoretical model (STM) is:

$$V_{stm}(n) = \left( \frac{E_0}{t_d} \right)^{0.5} \left( \frac{1}{R_{load}} + \frac{n}{R_0} \right)^{-0.5} \quad (5.10)$$

where  $t_d$  is the duration of the event,  $E_0$  is energy captured at impact mechanism, and  $n$  is the number of devices.

The efficiency of the device is broken down into two stages; impact mechanism and mechoelectric conversion mechanism.

### 5.3.4.1 Impact Mechanism Efficiency

Using the STM (from Chapter 4) and Equation 5.10 with the experimental data empirically model in Equation 5.9 the energy captured from the impact mechanism  $E_0$  can be found. This is the energy transferred from the droplet to the harvester as the droplet impacts the surface.

Using the data from the experiments for the velocity of droplet at 2.13 m/s,  $V_{stm}(0)$  is found to be  $2.106 \pm 0.11$  V. Given that the whole harvesting process duration is  $t_0$ , estimated at 0.06 s,  $E_0$  is found to be  $266.2 \pm 29$  nJ. Table 5.1 gives values for the kinetic energy of drops, and thus the efficiency of the impact mechanism can be estimated and is found to be  $0.350 \pm 0.054$  percent.

### 5.3.4.2 *Mechanoelectric Conversion Mechanism Efficiency*

Again, using the STM (from Chapter 4) and its Equation 5.10 with the experimental data empirically model in Equation 5.9 and also knowing the energy captured from the impact mechanism  $E_0$ , the losses within a harvest  $R_0$  can be found. This is realized by using a numerical method by inputting trial values of  $R_0$  in Equation 5.10 to find best fit to the experimental data empirically model by Equation 5.9.

The energy delivered by a single device is found to be  $51 \pm 12$  nJ. This energy comes from the energy delivered by the impact mechanism which is  $266.2 \pm 29$  nJ, giving an efficiency for the mechnoelectric conversion mechanism of  $0.334 \pm 0.073$  percent.

### 5.3.5 CONCLUSION

This overall study investigates an alternative approach to harvesting energy with piezoelectric materials by utilizing raindrop impacts. Detailed experimental results with distinct features are presented, highlighting the log growth and exponential decay of the harvesting process of a droplet impact. It has been shown that the droplet impact stage has a significant contribution to the overall power output of the device.

This study has demonstrated the detailed behavior of a harvesting system, scavenging energy from raindrop impacts. Three main findings of the first part of the work are:

- The detailed voltage output profile from the piezoelectric device shows that there is an impact stage during the droplet impact process, followed by a decay stage as stored energy in the harvester is dissipated, with an oscillatory character to the harvesting event of an impact.
- The impact stage lasts for a significant time period when compared to the duration of the entire harvesting event and has a significant amount of energy associated with it.
- The power output is very small and is consistent with the findings of other researchers. Nonetheless, the efficiency is found to be very small also, providing an opportunity for future improvement of the transfer function of the device, for example, by modifying the harvester's surface.

Three main findings of the second part of the work are:

- A technique is found to separate the efficiency of the impact mechanism as the droplet interacts with the device and the efficiency of the mechanoelectric conversion mechanism due to internal losses in the device.
- Values for the impact mechanism efficiency and the conversion mechanism efficiency.
- The optimum arrangement for a single device.



## CHAPTER 6

---

# CONCLUSION

As the technology matures, the focus will shift to the new applications to be able to integrate the harvesters into existing systems. This will lead to development of low-power electronics (to minimize power losses) and wireless communications. The cost of energy harvesters will dramatically fall over a period of time and support the development of energy harvesting devices. Some of the commercial applications can include industrial condition monitoring, powering remote infrastructure, and wireless sensor networks.

### 6.1 CHALLENGES

Most prior structures utilize the bending strain of cantilever beams at resonance condition to generate electrical power using piezoelectric materials. However, one of the challenges is that we gain smaller power output than the theoretical power predicted. Moreover, the resonant frequency of conventional piezoelectric energy harvesters is very high and the bandwidth too narrow, which prevents the application of such devices where diverse range of frequencies is substantial.

Some of the suggested improvements would be:

- the impact mechanism's efficiency by surface modifications techniques,
- mechanical–electrical conversion efficiency by controlled micro-fabrication techniques,
- the array connection efficiency by low-voltage drop rectification,
- integration of impact harvester with other sources (e.g., photovoltaic cell to produce a combined harvester module), and
- optimization for specialist applications.

Powering medical devices that are isolated from power supplies, perhaps sophisticated implants, and powering patch-type health care devices are examples of where harvesting power units can be used to bring societal benefits. In terms of scientific impact, significant work is still needed on developing the understanding of degradation mechanisms of piezoelectric materials. Reliability publications are needed to be able to successfully implement harvesting technologies with confidence, particularly in the medical arena or other critical applications.

## 6.2 FUTURE PROSPECTS

There are many possible improvements to lead zirconate titanate (PZT) materials to lower the frequencies and widening their bandwidth. Research is on-going to develop a low-cost and commercial method to overcome these problems, especially with PZT materials. The research should focus on achieving and maintaining maximum power point.

Materials such as PZT have the constraint of low flexibility and low piezoelectric property. Future electronic applications, substrate, and piezoelectric materials are required to have the freedom in shapes with flexible, transparent, and stretchable characteristics. The future research will be able to position itself in various applications beyond mobile or handheld devices, for example, patch-type health care devices and wearable energy-generating sources for flexible electronics. Therefore, new organic-based piezoelectric materials for flexible energy harvester are required with high piezoelectricity property and sustainable material property.

The ambition would be to improve particular properties of organic piezoelectrics to achieve energy-gleaning efficiencies and life expectancy for sustainable flexibility, which are significantly better than PZT. To further explore these critical factors that influence the sustainability of the piezoelectric and electrode properties for a prescribe duration further work needs to be carried out.

# REFERENCES

- [1] Calhoun, B., D. Daly, and N. Verma. 2005. "Design Considerations for Ultra-Low Energy Wireless Microsensor Nodes." *IEEE Transactions on Computers* 54, no. 6, pp. 727–40.
- [2] Hajati, A., and S.G. Kim. 2011. "Ultra-Wide Bandwidth Piezoelectric Energy Harvesting." *Applied Physics Letters* 99, no. 8.
- [3] Vullers, R.J.M., R. Schaijk, I. Doms, C. Van Hoof, and R. Mertens. 2009. "Micropower Energy Harvesting." *Solid State Electronics* 53, no. 7, pp. 684–93.
- [4] Cook, J.W., S. Lanzisera, and K.S. Pister. 2006. "SoC Issues for RF Smart Dust." In *Proceedings of IEEE* 94, no. 6, pp. 1177–96.
- [5] Mitcheson, P.D., E.M. Yeatman, G.K. Rao, A.S. Holmes, and T.C. Green. 2008. "Energy Harvesting from Human and Machine Motion for Wireless Electronic Devices." In *Proceedings of IEEE* 96, no. 9, pp. 1457–86.
- [6] Raju, M. 2008. "Energy Harvesting: ULP Meets Energy Harvesting." Texas Instruments White Paper.
- [7] Harrop, P., and H. Zervos. 2017. "Energy Harvesting: Off-Grid Microwatt to Megawatt 2017–2027." IDTechEx.
- [8] Williams, C.B., and R.B. Yates. 1996. "Analysis of a Micro-Electric Generator For Microsystems." *Sensors and Actuators A* 52, nos. 1–3, pp. 8–11.
- [9] Soliman, M.S.M., and E.F. El-Saadany. July 13, 2006. "Electromagnetic MEMS Based Micro-Power Generator." *IEEE International Symposium on Industrial Electronics* 4, pp. 2747–53.
- [10] Kazmierski, T.J., and S. Beeby. 2011. *Energy Harvesting Systems—Principles, Modelling and Applications*. New York, NY: Springer.
- [11] Reily, E.K., F. Burghardt, R. Fain, and P. Wright. 2011. "Powering a Wireless Sensor Node with a Vibration-Driven Piezoelectric Energy Harvester." *Smart Materials and Structures* 20, no. 12.
- [12] Trolrier-Mckinstry, S., and P. Muralt. 2004. "Thin Film Piezoelectrics for MEMS." *Journal of Electroceramics* 12, no. 1, pp. 7–17.
- [13] Ottaman, G.K., A.C. Bhatt, H. Hofmann, and G.A. Lesieutre. 2002. "Adaptive Piezoelectric Energy Harvesting Circuit for Wireless Remote Power Supply." *IEEE Transaction on Power Electronics* 17, no. 5, pp. 669–76.
- [14] Zakar, E. 2004. *MEMS Piezo Pressure Sensor for Military Applications*. Adelphi, MD: U.S. Army Research Laboratory.
- [15] Tilmans, H.A.C. 1996. "Equivalent Circuit Representation of Electromechanical Transducers: I.Lumped-Parameter Systems." *Micromechanics and Microengineering* 6, no. 1, pp. 157–76.

- [16] Lipscomb, I.P., P.M. Weaver, J. Swingler, and J.W. McBride. 2009. "The Effect of Relative Humidity, Temperature and Electrical Field on Leakage Currents in Piezo-Ceramic Actuators Under DC Bias." *Sensors and Actuators A: Physical* 151, no. 2, pp. 179–86.
- [17] Lipscomb, I.P., P.M. Weaver, J. Swingler, and J.W. McBride. 2009. "Micro-Computer Tomography-An Aid in the Investigation of Structural Changes in Lead Zirconate Titanate Ceramics After Temperature-Humidity Bias Testing." *Journal of Electroceramics* 23, no. 1, pp. 72–75.
- [18] Rocha, J., L. Gonclaves, P. Rocha, and S. Lanceros-Mendez. 2010. "Energy Harvesting from Piezoelectric Materials Fully Integrated in Footwear." *IEEE Transactions on Industrial Electronics* 57, no. 3, pp. 813–19.
- [19] Ramer, N., T. Marrone, and A. Stiso. 2006. "Structure and Vibrational Frequency Determination for  $\alpha$ -poly(Vinylidene Fluoride) Using Density-Functional Theory." *Polymer* 47, no. 20, pp. 7160–65.
- [20] Roundy, S., P. Wright, and J. Rabaey. 2003. *Energy Scavenging for Wireless Sensor Networks with Special Focus on Vibrations*. Norwell, MA: Kluwer Academic Press.
- [21] Xu, C.N., M. Akiyama, K. Nonaka, and T. Watanabe. 1995. "Intelligent Ceramic Materials: Issues of Brittle Fracture." *Journal of Intelligent Material Systems and Structures* 6, no. 1, pp. 49–54.
- [22] Roundy, S., P.K. Wright, and J. Rabaey. 2003. "A Study of Low Level Vibrations as a Power Source for Wireless Sensor Nodes." *Computer Communications* 26, no. 11, pp. 1131–44.
- [23] Roundy, S., and P.K. Wright. 2004. "A Piezoelectric Vibration Based Generator for Wireless Electronics." *Smart Materials and Structures* 13, no. 5, pp. 1131–42.
- [24] Mavrokefalos, A., A.L. Moore, M.T. Pettes, L. Shi, W. Wang, and X. Li. 2009. "Thermoelectric and Structural Characterizations of Individual Electrodeposited Bismuth Telluride Nanowires." *Journal of Applied Physics* 105, no. 10.
- [25] Zaitsev, V.K., M.I. Fedorov, and E.A. Gurieva. 2005. "Thermoelectrics of N-type with  $ZT > 1$  Based on Mg/sub 2/Si-Mg/sub 2/Sn Solid Solutions." In *ICT 24th International Conference on Thermoelectrics*, Clemson.
- [26] Janak, L., Z. Ancik, J. Vetiska, and Z. Hadas. 2015. "Thermoelectric Generator Based on MEMS Module as an Electric Power Backup in Aerospace Applications." In *12th European Conference on Thermoelectrics*, Madrid.
- [27] Ding, L.C., N. Meyerheinrich, L. Tan, K. Rahaoui, R. Jain, and A. Akbarzadeh. 2017. "Thermoelectric Power Generation from Waste Heat of Natural Gas Water Heater." In *ICEP 1st International Conference on Energy and Power*, Melbourne.
- [28] Jo, S.E., M.S. Kim, M.K. Kim, H.L. Kim, and Y.J. Kim. 2012. "Human Body Heat Energy Harvesting Using Flexible Thermoelectric Generator for Autonomous Microsystems." In *16th International Conference on Miniaturized systems for Chemistry and Life Sciences*, Okinawa.

- [29] Salmi, T., M. Bouzguenda, A. Gastli, and A. Masmoudi. 2012. "Matlab/Simulink Based Modelling of Solar Photovoltaic Cell." *International Journal of Renewable Energy Research* 2, no. 2, pp. 213–18.
- [30] Nema, S., R.K. Nema, and G. Agnihotri. 2010. "Matlab/Simulink Based Study of Photovoltaic Cells, Modules, Array and their Experimental Verification." *International Journal of Energy and Environment* 1, no. 3, pp. 487–500.
- [31] Hernandez, J.C., J. Cruz De La, and B. Ogayar. 2012. "Electrical Protection for the Grid-Interconnection of Photovoltaic-Distributed Generation." *Electric Power Systems Research* 89, pp. 85–99.
- [32] Dubey, S., G. Tiwari, and D. Mills. 2008. "Thermal Modelling of a Combined System of Photovoltaic Thermal (PV/T) Solar Water Heater." *Solar Energy* 82, no. 7, pp. 612–12.
- [33] Chow, T. 2010. "A Review on Photovoltaic/Thermal Hybrid Solar Technology." *Applied Energy* 87, no. 2, pp. 365–79.
- [34] Zondag, H. 2008. "Flat-Plate PV-Thermal Collectors and Systems: A review." *Renewable and Sustainable Energy Reviews* 12, no. 4, pp. 891–959.
- [35] Dupeyrat, P., C. Menezo, H. Wirth, and M. Rommel. 2011. "Improvement of PV Module Optical Properties for PV-thermal Hybrid Collector Application." *Solar Energy Materials and Solar Cells* 95, no. 8, pp. 2028–36.
- [36] Deng, Y., W. Zhu, Y. Wang, and Y. Shi. 2013. "Enhanced Performance of Solar-Driven Photovoltaic-Thermoelectric Hybrid System in an Integrated Design." *Solar Energy* 88, pp. 182–91.
- [37] Liao, T., B. Lin, and Z. Yang. 2014. "Performance Characteristics of a Low Concentrated Photovoltaic-Thermoelectric Hybrid Power Generation Device." *International Journal of Thermal Sciences* 77, pp. 158–64.
- [38] Khasee, N., C. Lertsatitthanokorn, and B. Bubphachot. 2013. "Energy and Exergy Analysis of a Double-Pass Thermoelectric Solar Air Collector." *International Journal of Exergy* 12, no. 1.
- [39] Jarnagin, W. 1986. "Integrated PV-thermal Panel and Process for Production." United States Patent Application Number 4607132.
- [40] Ansley, J., J. Botkin, and T. Dinwoodie. 2004. "PV/Thermal Solar Power Assembly." United States Patent Application Number 6675580.
- [41] Aurelienr, P.Z.T. 2015. Application Manual, [Online]. Available at <http://aurelienr.com/electronique/piezo/piezo.pdf>
- [42] Shenck, N.S., and J.A. Paradiso. 2001. "Energy Scavenging with Shoe-Mounted Piezoelectrics." *IEEE Micro* 21, no. 3, pp. 30–42.
- [43] Wojcik, G.L., D.K. Vaughan, N. Abboud, and J. Mould. 1993. "Electromechanical Modeling Using Explicit Time-Domain Finite Elements." in *IEEE Ultrasonics Symposium Proceedings*.
- [44] AZoM Network. 2001. "Piezoelectric Materials—An Overview." Retrieved from [www.azom.com](http://www.azom.com)
- [45] Erturk, A., and D.J. Inman. 2011. *Piezoelectric Energy Harvesting*. Hoboken, NJ: John Wiley and Sons, Ltd.

- [46] Jaffe, B., W. Cook, and H. Jaffe. 1971. *Piezoelectric Ceramics*. Cambridge, MA: Academic Press.
- [47] Lee, H.J., and D.A. Saravanos. 1997. *The Effect of Temperature Dependent Material Nonlinearities on the Response of Piezoelectric Composite Plates*. Lewis Research Center, NASA.
- [48] Ajitsaria, J.K. 2008. *Modelling and Analysis of PZT Micropower Generator*. Auburn, AL: Auburn University.
- [49] Weaver, P.M., M.G. Cain, A. Anson, J. Franks, I.P. Lipscomb, J.W. McBride, and D. Zheng. 2012. "The Effects of Porosity, Electrode and Barrier Materials on the Conductivity of Piezoelectric Ceramics in High Humidity and dc Electric Field." *Smart Materials and Structures* 21, no. 4.
- [50] Howells, C.A. 2009. "Piezoelectric Energy Harvesting." *Energy Conversion and Management* 50, pp. 1847–50.
- [51] Ando, M. 2012. "Organic Piezoelectric Film Reshapes Sensor Features," Murata.
- [52] Zakharov, D., B. Gusarov, B. Gusarova, B. Viala, O. Cugat, J. Delamare, and L. Gimeno. 2013. "Combined Pyroelectric, Piezoelectric and Shape Memory Effects for Thermal Energy Harvesting." *Journal of Physics: Conference Series* 476, no. 1.
- [53] Park, K., S. Shin, A. Tazebay, H. Um, J. Jung, S. Jee, M. Oh, S. Park, B. Yoo, C. Yu, and J. Lee. 2013. "Lossless Hybridization Between Photovoltaic and Thermoelectric Devices." *Scientific Reports* 3.
- [54] Wang, N., L. Han, H. He, N.H. Park, and K. Koumoto. 2011. "A Novel High-Performance Photovoltaic–Thermoelectric Hybrid Device." *Journal of Energy and Environmental Science* 4, no. 9, pp. 3676–79.
- [55] Van Sark, W. 2011. "Feasibility of Photovoltaic—Thermoelectric Hybrid Modules." *Journal of Applied Energy* 88, no. 8, pp. 2785–90.
- [56] Zhang, Y., J. Fang, C. He, H. Yan, Z. Wei, and Y. Li. 2013. "Integrated Energy-Harvesting System by Combining the Advantages of Polymer Solar Cells and Thermoelectric Devices." *The Journal of Physical Chemistry C* 117, no. 47, pp. 24685–91.
- [57] The Institute of Electrical and Electronic Engineers. 1988. "IEEE Standards on Piezoelectricity." *IEEE Standards*.
- [58] Blevings, R.D. 1980. "Formulas for Natural Frequency and Mode Shape." *The Journal of the Acoustical Society of America* 67.
- [59] Ilyas, M.A. 2013. "Piezoelectric Energy Harvesting." *MSc Dissertation submitted to Heriot-Watt University*.
- [60] Biswas, P., M. Uddin, M. Islam, M. Sarkar, V. Desa, M. Khan, and A. Huq. 2009. "Harnessing Raindrop Energy in Bangladesh." In *International Conference on Mechanical Engineering*, Dhaka.
- [61] Guigon, R., J. Chailout, T. Jager, and G. Despesse. 2008. "Harvesting Raindrop Energy: Theory." *Smart Materials and Structures* 17, no. 1.
- [62] Guigon, R., J. Chailout, T. Jager, and G. Despesse. 2008. "Harvesting Raindrop Energy: Experimental Study." *Smart Materials and Structures* 17, no. 1.

- [63] Viola, F., P. Romano, R. Miceli, and G. Acciari. 2013. "Harvesting Rainfall Energy by Means of Piezoelectric Transducer." In *International conference on Clean Electrical Power*, Alghero.
- [64] Chin-Hong, W., Z. Dahari, A. Abd Manaf, O. Sidek, M. Miskam, and J. Mohamed. 2013. "Simulation of Piezoelectric Raindrop Energy Harvester." In *TENCON*, Sydney.
- [65] Wong, C.H., Z. Dahari, A.A. Manaf, and M.A. Miskam. 2015. "Harvesting Raindrop Energy with Piezoelectrics: A Review." *Journal of Electronic Materials* 44, no. 1, pp. 13–21.
- [66] Nayan, N.M., M.F.A. Razak, A. Ali, S.K. Mazalan, A.N.N. Abdullah, and N.H. Rahman. 2015. "Development of Rain Harvester Using Piezoelectric Sensor." In *International Conference on Power, Energy and Communication Systems*, Perlis.
- [67] Viola, F., P. Romano, R. Miceli, and G. Acciari. 2013. "Harvesting Rainfall Energy by Means of Piezoelectric Transducers." In *Clean Electrical Power*, Alghero.
- [68] LEO, R.D., V. Massimo, F. Gianluca, and L. Lecce. 2013. "Preliminary Theoretical Study About a 'Piezoelectric Shingle' for a Piezoelectric Energy Harvesting System in Presence of Rain." *Mathematical and Computational Methods in Electrical Engineering*, pp. 9–17.
- [69] Shan, X., R. Song, B. Liu, and T. Xie. 2015. "Novel Energy Harvesting: A Macro Fiber Composite Piezoelectric Energy Harvester in the Water Vortex." *Ceramic International* 41, pp. 7633–767.
- [70] Song, R., X. Shan, F. Lv, and T. Xie. 2015. "A Study of Vortex-Induced Energy Harvesting from Water Using PZT Piezoelectric Cantilever with Cylindrical Extension." *Ceramics International* 41, pp. 768–73.
- [71] Martin, R. 1993. "Phenomena of Liquid Drop Impact on Solid and Liquid Surfaces." *Fluid Dynamics Research* 12, no. 2, pp. 61–93.
- [72] Rein, M. 2002. *Drop-surface Interactions*. New York, NY: Springer.
- [73] Perera, K., B. Sampath, V. Dassanayake, and B. Hapuwatte. 2014. "Harvesting of Kinetic Energy of the raindrops." *International Journal of Mathematical, Computational, Physical and Quantum Engineering* 8, no. 2, pp. 325–30.
- [74] Stow, C., and M. Hadfield. 1981. "An Experimental Investigation of Fluid Flow Resulting from the Impact of a Water Drop with an Unyielding Dry Surface." In *Royal Society A:Mathematical Physical and Engineering Sciences*.
- [75] Mundo, C., M. Sommerfeld, and C. Tropea. 1995. "Droplet-Wall Collisions: Experimental Studies of the Deformation and Break-Up Processes." *International Journal of Multiphase Flow* 21, no. 2, pp. 151–73.
- [76] Josserand, C., and S. Zaleski. 2003. "Droplet Splashing on a Thin Liquid Film." *Physics of Fluids* 15, no. 6, pp. 1650–57.
- [77] Sikalo, S., M. Marengo, C. Tropea, and E. Ganic. 2002. "Analysis of Impact of Droplets on Horizontal Surfaces." *Experimental Thermal and Fluid Sciences* 25, no. 7, pp. 503–10.

- [78] Sikalo, S., C. Tropea, and E. Ganic. 2005. "Impact of Droplets Onto Inclined Surfaces." *Journal of Colloid and Interface Science* 286, no. 2, pp. 661–69.
- [79] Robert, H. 1997. "Stratiform Precipitation in Regions of Convection: A Meteorological Paradox?" *Bulletin of the American Meteorological Society* 78, no. 10, pp. 2179–96.
- [80] Ilyas, M.A., and J. Swingler. 2015. "Piezoelectric Energy Harvesting from Raindrop Impacts." *Energy* 90, no. 1, pp. 796–806.
- [81] Aboud, D.G.K., and A.M. Kietzig. 2015. "Splashing Threshold of Oblique Droplet Impacts on Surfaces of Various Wettability." *Langmuir* 31, no. 36, pp. 10100–111.
- [82] Liu, J., H. Vu, S. Yoon, R. Jepsen, and G. Aguilar. 2010. "Splashing Phenomena During Liquid Droplet Impact." *Atomization and Sprays* 20, no. 4, pp. 297–310.
- [83] Ilyas, M.A., and J. Swingler. 2017. "Towards a Prototype Module for Piezoelectric Energy Harvesting from Raindrop Impacts." *Energy* 125, pp. 716–25.

# ABOUT THE AUTHOR

**Mohammad Adnan Ilyas** is a doctoral researcher at Heriot-Watt University, UK. He received a BEng (Hons) in Electrical and Electronic Engineering in 2012, followed by an MSc in Renewable Energy and Distributed Generation in 2013. His research interests includes renewable energy with a focus on piezoelectric energy harvesters, energy efficiency and storage.



# INDEX

## A

Autonomous energy system, 4–6

## B

Battery-operated devices, power consumption of, 3

## C

Circuit topologies

  full-bridge rectifier, 26–27

  voltage doubler, 26–27

Combined energy harvesting

  future trends and commercial patents, 16

  review and background, 14–15

Converse effect, 18

## D

Direct piezoelectric effect, 18

## E

Electromagnetic generators, 7

Electrostatic generators, 8

Energy harvesting

  benefits of, 4

  combined, 14–16

  description of, 3–4

  energy fields, 4

  photovoltaic, 13–14

  thermoelectric, 10–13

  vibrational, 6–10

## F

Faraday's law, 7

Ferroelectric ceramics, 19–20

Figure of merit, 11–12

Full-bridge rectifier, 26–27

## H

Harvester characteristics

  impact mechanism, 35–37

  impact velocity, 34

  surface interaction, 37–39

## I

Impact mechanism, 35–37

Impact velocity, 34

## M

Modeling, 23–25

## O

Organic materials, 20

## P

Photovoltaic energy harvesting, 13–14

Piezoelectric constant materials, 19

Piezoelectric energy harvesting systems

  challenges, 47–48

  circuit topologies, 25–27

- full-bridge rectifier, 26–27
- voltage doubler, 26–27
- electrical behavior, 25
- experimental work, 26–29
- future prospects, 48
- mechanical behavior, 25
- modeling, 23–25
- Piezoelectric generators, 9–10
- Piezoelectric materials
  - description of, 18–19
  - ferroelectric ceramics, 19–20
  - future prospects, 20–21
  - organic materials, 20
- R**
- Raindrop energy harvesting (REH)
  - experimental setup
    - device efficiency, 42–44
    - multiple device, 42
    - single device, 41–42
    - voltage profile, 39–41
  - harvester characteristics
    - impact mechanism, 35–37
    - impact velocity, 34
    - surface interaction, 37–39
    - review of publications, 31–34
- REH. *See* Raindrop energy harvesting
- S**
- Seebeck coefficient, 11
- Surface interaction, 37–39
- T**
- TEG. *See* Thermoelectric generator
- Thermoelectric energy harvesting, 10–13
- Thermoelectric generator (TEG), 10–13
- Transducers, 11
- V**
- Vibrational energy harvesting
  - components of, 6–7
  - electromagnetic, 7
  - electrostatic, 8
  - piezoelectric, 9–10
  - summary of generators, 10
- Voltage doubler, 26–27

## OTHER TITLES IN OUR ENERGY PHYSICS AND ENGINEERING COLLECTION

Jonathan Swingler, Editor

---

*Einstein's Mass-Energy Equation, Volume I: Early History and  
Philosophical Foundations*  
by Francisco Fernflores

*Einstein's Mass-Energy Equation, Volume II: Quantum Mechanics  
and Gravitation, Empirical Tests, and Philosophical Debates*  
by Francisco Fernflores

*Utilization of Variable Energy Sources*  
by Wolf-GerritFrüh

*Electrical Power and Energy: Transformers, Synchronous  
Machines, and Power Networks*  
by Siong Lee Koh

*Energy in Electrical Fields*  
by Paul Weaver

Momentum Press is one of the leading book publishers in the field of engineering, mathematics, health, and applied sciences. Momentum Press offers over 30 collections, including Aerospace, Biomedical, Civil, Environmental, Nanomaterials, Geotechnical, and many others.

Momentum Press is actively seeking collection editors as well as authors. For more information about becoming an MP author or collection editor, please visit <http://www.momentumpress.net/contact>

---

### Announcing Digital Content Crafted by Librarians

Momentum Press offers digital content as authoritative treatments of advanced engineering topics by leaders in their field. Hosted on ebrary, MP provides practitioners, researchers, faculty, and students in engineering, science, and industry with innovative electronic content in sensors and controls engineering, advanced energy engineering, manufacturing, and materials science.

#### **Momentum Press offers library-friendly terms:**

- perpetual access for a one-time fee
- no subscriptions or access fees required
- unlimited concurrent usage permitted
- downloadable PDFs provided
- free MARC records included
- free trials

The **Momentum Press** digital library is very affordable, with no obligation to buy in future years.

For more information, please visit [www.momentumpress.net/library](http://www.momentumpress.net/library) or to set up a trial in the US, please contact [mpsales@globalepress.com](mailto:mpsales@globalepress.com).



**EBOOKS  
FOR THE  
ENGINEERING  
LIBRARY**

*Create your own  
Customized Content  
Bundle — the more  
books you buy,  
the higher your  
discount!*

**THE CONTENT**

- *Manufacturing Engineering*
- *Mechanical & Chemical Engineering*
- *Materials Science & Engineering*
- *Civil & Environmental Engineering*
- *Electrical Engineering*

**THE TERMS**

- *Perpetual access for a one time fee*
- *No subscriptions or access fees*
- *Unlimited concurrent usage*
- *Downloadable PDFs*
- *Free MARC records*

**For further information,  
a free trial, or to order,  
contact:  
sales@momentumpress.net**

# **Piezoelectric Energy Harvesting**

*Methods, Progress, and Challenges*

**Mohammad Adnan Ilyas**

Environmental pollution has been one of the main challenges for sustainable development. Piezoelectric materials can be used as a means of transforming ambient vibrations into electrical energy to power devices. The focus is on an alternative approach to scavenge energy from the environment. This book presents harvesting methodologies to evaluate the potential effectiveness of different techniques and provides an overview of the methods and challenges of harvesting energy using piezoelectric materials.

Piezoelectric energy harvesters have many applications, including sensor nodes, wireless communication, microelectromechanical systems, handheld devices, and mobile devices. The book also presents a new approach within piezoelectric energy harvesting using the impact of raindrops. The energy-harvesting model presented is further analyzed for single-unit harvester and an array of multiple harvesters to maximize the efficiency of the device.

**Mohammad Adnan Ilyas** received a bachelor of engineering (Hon) in electrical and electronic engineering from Heriot-Watt University, UK, in 2012 followed by an MSc in renewable energy and distributed generation in 2013. Currently Adnan is pursuing his research in energy harvesting with a focus on piezoelectrical harvesters to obtain a PhD in electrical engineering at Heriot-Watt University, UK.



**MOMENTUM PRESS  
ENGINEERING**

